Biological Journal of the Linnean Society, 2020, **130**, 268–295. With 11 figures.

Bone histology yields insights into the biology of the extinct elephant birds (Aepyornithidae) from Madagascar

ANUSUYA CHINSAMY[1,*], DELPHINE ANGST[1,2], AURORE CANOVILLE[3,4] and URSULA B. GÖHLICH[4,5]

[1]*University of Cape Town, Department of Biological Sciences, Private Bag X3, Rhodes Gift 7700, South Africa*
[2]*University of Bristol, School of Earth Sciences, Life Sciences Building, 24 Tyndall Avenue, Bristol BS8 1TQ, UK*
[3]*Paleontology, North Carolina Museum of Natural Sciences, 11 W. Jones Street, Raleigh NC 27601, USA*
[4]*Department of Biological Sciences, North Carolina State University, 3510 Thomas Hall, Raleigh NC 27695, USA*
[5]*Natural History Museum Vienna, Department of Geology and Paleontology, Burgring 7, 1010 Vienna, Austria*

Received 7 January 2020; accepted for publication 27 January 2020

Given that the biology of the recently extinct aepyornithids is poorly understood, we undertook a histological study of 29 skeletal elements of adult and juvenile specimens of Aepyornithidae, i.e. *Aepyornis maximus*, *Aepyornis hildebrandti* and *Vorombe titan*, in addition to a group of taxonomically unidentifiable juvenile Aepyornithiformes. Comparative analysis of the histology of the different skeletal elements showed that although the femur retained a good record of growth during early ontogeny, the tibiotarsus provided the best record of growth. Our data showed that, like other insular birds and their extant relative, the kiwi, Aepyornithidae experienced protracted growth. We also found that intracortical remodelling began early in ontogeny and continued throughout their lives, becoming more extensive throughout the compacta with age, albeit more restricted to the perimedullary region in the femora. We also deduced that the different skeletal elements experienced variable amounts of intracortical remodelling, which was most likely to be related to biomechanical constraints, size of the element and ontogenetic age. Additionally, we documented the occurrence of an unusual endosteal tissue within the large perimedullary erosional spaces of a femur of *A. maximus*. Overall, our study provided a lot of new information about the life history of these giant, recently extinct ratites.

ADDITIONAL KEYWORDS: bone remodelling – insular birds – ontogeny – Palaeognathae – protracted growth – terrestrial birds.

INTRODUCTION

Ostriches are the largest among modern terrestrial avifauna, reaching heights of ~2.5 m (including their necks) and body weights ≤ 150 kg (Deeming, 1999). However, the fossil record of birds bears testament to a diverse array of even larger terrestrial birds, such as *Dromornis stirtoni* from Australia and the elephant bird *Vorombe titan* from Madagascar. Both these birds attained heights of ~3 m, and an average body mass of 650 kg has been estimated for male specimens of *Dromornis* (Handley *et al.*, 2016) and the genus *Vorombe* (Hansford & Turvey, 2018).

Aepyornithid specimens have been recovered from several localities in Madagascar that span a time range from the Pleistocene to the Holocene (Angst & Buffetaut, 2017). Radiometric dating using eggshells has suggested more precise dates of ~2000–5000 years (Wetmore, 1967; Berger *et al.*, 1975; Tattersall, 1987; Burney *et al.*, 1997; Hansford & Turvey, 2018). There have been probable sightings during the French occupation of Madagascar in the 17th century, but these are not verifiable (Fuller, 1987). Intriguingly,

*Corresponding author. E-mail: anusuya.chinsamy-turan@uct.ac.za

some vegetation types in Madagascar today show widely spaced and small leaves, in addition to typical springy stems for the so-called wire plants (Bond & Silander, 2007). These features are hypothesized to be anachronistic defence structures against elephant bird browsing, suggestive of a long co-evolutionary history between these animals and plants.

In the early days after their discovery, Aepyornithidae were subjected to considerable taxonomic evaluations. The species *Aepyornis maximus* was first established in 1851 by Geoffrey Saint-Hilaire based on an isolated and complete egg. This original description (Geoffrey Saint-Hilaire, 1851) was followed by a number of morphological studies in the late 19th and early 20th centuries that described osteological remains attributed to the potential layers of such a large egg. These studies resulted in the naming of several new *Aepyornis* species (for an overview, see Hansford & Turvey, 2018), in addition to the establishment of another aepyornithid genus, *Mullerornis*, representing smaller and more lightly built individuals (Geoffrey Saint-Hilaire, 1851; Burckhardt, 1893; Andrews, 1894a, b, 1896, 1897; Pycraft, 1900; Monnier, 1913; Wiman, 1935, 1937a, b). Monnier (1913) recognized four species for the genus *Aepyornis*: a large form, *A. maximus* (Geoffrey Saint-Hilaire, 1851), and three medium-sized ones, *Aepyornis medius* (Milne-Edwards & Grandidier, 1869), *Aepyornis hildebrandti* (Burckhardt, 1893) and *Aepyornis gracilis* (Monnier, 1913). Hansford & Turvey (2018) conducted the most recent taxonomic evaluation of elephant birds (Aepyornithidae) from Madagascar. On the basis of linear morphometrics data of appendicular elements, these researchers recognized three distinct skeletal morphotypes (Hansford & Turvey, 2018): (1) a small-bodied morphotype, represented by the genus *Mullerornis*; (2) a medium-bodied morphotype, represented by the genus *Aepyornis*, within which two species, *A. hildebrandti* and *A. maximus*, were identified; and (3) a large-bodied morphotype, represented by the genus *Vorombe*.

The Aepyornithidae share many plesiomorphic characters with kiwi and tinamous and have therefore been considered to be basal ratites (Cracraft, 1974). Recent DNA studies have confirmed that *Aepyornis* is a ratite and that its closest living relative is *Apteryx*, the New Zealand kiwi (Mitchell *et al.*, 2014). Given that Madagascar and New Zealand were never connected directly, these researchers proposed that there must have been a flighted ancestor that facilitated such long-distance dispersal. In New Zealand, the large body size niche was already filled by the moa (Dinornithidae); therefore, being small might have been an adaptive strategy for the kiwi.

Complete (i.e. intact) *Aepyornis* eggs are rare and are known to have volumes of 5.6–13 L (Amadon, 1947; Balanoff & Rowe, 2007; Angst *et al.*, 2014), with lengths of ~26–40 cm and widths of 19–25 cm (Geoffroy Saint-Hilaire, 1851; Lavauden, 1931; Henrici, 1957; Mlíkovský, 2003). In 1967, Wetmore (1967) scanned an intact *Aepyornis* egg and published the first account of an embryo therein. However, the image resolution was too low to permit detailed anatomical analysis of the embryo. Subsequently, Balanoff & Rowe (2007) scanned the so-called 'National Geographic *Aepyornis* egg' using high-resolution X-ray computed tomography and provided the first detailed morphological description of an *Aepyornis* embryo. The skeleton of the embryo was largely unfused and afforded the rare opportunity of detailed morphological descriptions of the skull bones, in addition to several postcranial elements. On the whole, the embryonic skeleton appeared to be even more robust than that of hatchlings of ostriches and rheas (Balanoff & Rowe, 2007), suggesting a hyper-precocial state at hatching for this group. By comparing the embryo with developmental stages of modern ostriches (*Struthio*), kiwi (*Apteryx*) and chickens (*Gallus*), these researchers determined that the embryo was 80–90% through incubation at the time of its death.

It is generally considered that at the end of the Pleistocene and the beginning of the Holocene considerable aridification resulted in a change from mainly C_3 plants to C_4 vegetation, which severely affected *Aepyornis* (Mahé & Sourdat, 1972; Burney, 1997; Rakotozafy & Goodman, 2005; Clarke *et al.*, 2006). These birds were finally pushed to extinction when the first humans arrived in Madagascar (~350 BC; Clarke *et al.*, 2006; Gommery *et al.*, 2011; Hansford & Turvey, 2018). It is thought that their enormous eggs (the largest of all amniotes known to date) were sought after by people, and their over-exploitation might have contributed to their demise (Clarke *et al.*, 2006; Gommery *et al.*, 2011). Although elephant birds overlapped with humans, we know hardly anything about their biology and life history. Given that the usefulness of fossil bone microstructure is now well recognized as providing pertinent information about the biology and growth strategy of extinct animals (e.g. Chinsamy-Turan, 2005; Erickson, 2005; Martinez-Maza *et al.*, 2014; Angst *et al.*, 2017), we undertook to investigate the bone histology of several specimens of aepyornithids to decipher various aspects of their life history.

Studies have shown that in most somatically mature neornithine birds, limb elements have a triple-layered bone wall consisting of outer and inner circumferential layers of bone tissue, which enclose a central region of primarily fibrolamellar bone (FLB) that can be remodelled partly or completely into Haversian bone during adulthood (Enlow & Brown, 1957; Chinsamy, 1995; Starck & Chinsamy, 2002; Chinsamy-Turan,

2005; de Ricqlès *et al.*, 2016; Watanabe, 2018). The central periosteal layer of bone is deposited during early ontogeny, while the skeletal elements grow in diameter. The outer circumferential layer (of periosteal origin) and inner circumferential layer (of endosteal origin) are deposited during later stages of ontogeny (Chinsamy, 1995; Ponton *et al.*, 2004; Watanabe, 2018). This pattern of bone tissue generally holds true for most birds that reach adult body size in < 1 year. However, exceptions to this growth pattern are seen in birds that are not under pressure to grow rapidly (Starck & Chinsamy, 2002), such as insular species. For example, Turvey *et al.* (2005) showed that the moa (Dinornithiformes) from New Zealand took several years to reach adult body size, and Bourdon *et al.* (2009) found that the small-bodied *Apteryx* (kiwi), also from New Zealand, can take ≤ 9 years to reach skeletal maturity. Likewise, the insular flightless bird *Pezophaps solitaria* (from La Réunion Island in the Mascarene; Steel, 2009) and the extinct Mesozoic *Gargantuavis* (Chinsamy *et al.*, 2014) from the Ibero-Armorican islands experienced slower, extended, cyclical growth to skeletal maturity.

De Ricqlès *et al.* (2016) provided the first histological assessment of five postcranial aepyornithid bones (which at the time were identified as four specimens of *A. maximus* and one of *A. medius*). Their study revealed that *Aepyornis* had well-vascularized FLB tissue, with cyclical growth marks in the cortices of at least two bones (de Ricqlès *et al.*, 2016). They also showed that secondary reconstruction could be intense in the perimedullary region of the bones they studied. A single femur of an aepyornithid (identified then as *A. maximus*) was included in another study that investigated whether osteohistological features in palaeognathous birds exhibited a phylogenetic signal (Legendre *et al.*, 2014). However, except for a sentence stating that the bone 'is seemingly fibrolamellar with a majority of circular canals', no other histological details of the '*Aepyornis*' femur were presented.

In the present study, we examine long bones (femora, tibiotarsi, fibulae and tarsometatarsi) of aepyornithid specimens identified at the species level: *A. maximus*, *A. hildebrandti* and *V. titan* (Table 1). In addition, we studied the histology of five juveniles and seven aepyornithid specimens that we were unable to assign to specific taxa (Table 1). Through this analysis we will assess the following factors: (1) possible ontogenetic changes in the bones assigned to taxa; (2) intraspecific variability in the skeletal elements studied; (3) which skeletal element(s) are more reliable for life-history reconstruction of these iconic giant extinct birds; and (4) whether the taxa can be distinguished from one another histologically.

MATERIAL AND METHODS

Osteological material

Twenty-nine disassociated aepyornithid skeletal elements were obtained for histological assessment (Table 1): 17 specimens (including five juveniles) were sampled from the collections of the Naturhistorisches Museum Wien, in Vienna, Austria (NHMW), and 12 adult bones came from the Muséum National d'Histoire Naturelle in Paris, France (MNHN).

As previously mentioned, the taxonomy of the Late Quaternary Aepyornithidae has been complicated notoriously by several debates about the validity of the different named species in the family (e.g. Hansford & Turvey, 2018). Hansford & Turvey (2018) have provided the most recent taxonomic assessment using morphometric data, and James Hansford personally used his large dataset to identify our specimens (Table 1). Thus, aside from the juvenile specimens that are difficult to diagnose to a species level and the few specimens that have insufficient data to permit valid identifications, the skeletal elements studied here belong to *A. maximus* (four tibiotarsi, two femora and one tarsometatarsus), *A. hildebrandti* (one femur and two tarsometatarsi) and *V. titan* (four tibiotarsi, one femur and two tarsometatarsi).

The small specimens (three tibiotarsi and two tarsometatarsi; Table 1) were recognized as juvenile individuals and not adults from the genus *Mulleornis* based on unfused epiphyses and metatarsal elements. More specifically, both sampled NHMW tibiotarsal specimens (2014/0238/0009 and 2014/0238/0015) have unfinished articular ends, while the tarsometatarsal (TMT) specimen (2014/0238/0048) has unfinished proximal and distal articular surfaces. Additionally, in comparison to adult specimens and other definite juveniles with unfused proximal ends, the distal trochleae are much less well defined and developed. For the tarsometatarsus (2014/0238/0049), only a part of the diaphysis is preserved, which gives no clear morphological indications of its juvenile status, but its relatively small size suggests that it was a young individual.

All the material from the NHMW and some of the specimens from the MNHN were recovered from the Antsirabe (also known as Antsirabé or Sirabé), a highland locality in central Madagascar ~100 km North of Antananarivo, which is one of the richest sites for aepyornithid material. The taphonomy and sedimentology of this locality suggest that it was a lake or at least a humid area, and it has been dated to the Pleistocene (~22 240 years before present; Goodman, 1999; Burney *et al.*, 2004; Goodman & Jungers, 2013). Climate data for Antananarivo shows strong seasonality, with wet winters, and minimum temperatures below 10 °C. Given that Antsirabe is at a slightly higher elevation, it would have been cooler and possibly wetter.

Table 1. Aepyornithid specimens studied, their anatomical measurements (in millimetres) and, where possible, their body mass (in kilograms)

Specimen number	Collection	Bone	Ontogenetic stage	Maximal length (mm)	Diaphysis minimal width (mm)	Diaphysis minimal circumference (mm)	Diaphysis depth (mm)	Width of proximal extremity (mm)	Cr-Cd length of proximal extremity (mm)	Diagonal length of proximal extremity (mm)	Width of distal extremity (mm)	Cr-Cd length of distal extremity (mm)	Diaphysis minimal circumference (mm)	BM based on femora (kg)	BM based on tibiotarsus (kg)
2014/0238/0015	NHMW	Tibiotarsus	Juvenile	–	37	101	22	–	–	–	–	–	101	–	86
2014/0238/0009	NHMW	Tibiotarsus	Juvenile	–	39	~106	23	103	60	–	–	–	~106	–	97
2014/0238/0017	NHMW	Tibiotarsus	–	–	50	~130	29	–	–	–	–	–	~130	–	159
2014/0238/0021	NHMW	Tibiotarsus	–	–	55	~145	33	–	–	–	111	–	~145	–	207
2014/0238/0016	NHMW	Tibiotarsus	–	–	–	–	–	152	85	–	–	–	–	–	–
TB3	MNHN	Tibiotarsus	–	–	–	–	–	168	–	–	–	–	–	–	–
TB2	MNHN	Tibiotarsus	–	–	–	–	–	164	–	–	–	–	–	–	–
TB7 (1937-62)	MNHN	Tibiotarsus	–	615	56	–	–	–	–	–	–	–	–	–	–
TB6 (1937-62)	MNHN	Tibiotarsus	–	670	57	160	42	175	100	–	120	80	160	–	262
TB4 (1937-62)	MNHN	Tibiotarsus	–	612	61	169	46	175	95	–	120	75	169	–	300
TB5 (1937-62)	MNHN	Tibiotarsus	–	645	61	173	45	180	100	–	130	90	173	–	317
TB1	MNHN	Tibiotarsus	–	–	–	190	–	–	–	–	–	–	190	–	398
TB8 (1937-62)	MNHN	Tibiotarsus	–	–	73	199	45	210	110	–	140	90	199	–	445
2014/0238/0052	NHMW	Femora	Juvenile	182	45	131	36	77	69	98	82	54	131	110	–
2014/0238/0038	NHMW	Femora	–	–	63	202	57	115	113	135	–	–	202	311	–
2014/0238/0047	NHMW	Femora	–	–	~64	~199	~55	124	128	–	–	–	~199	300	–
2014/0238/0046	NHMW	Femora	–	–	66	< 199	54	–	–	–	135	95	< 199	300	–
FM3 (MAD367 1906-17)	MNHN	Femora	–	350	81	244	81	157	148	160	155	85	244	491	–
FM2 (MAD 365)	MNHN	Femora	–	380	78	244	77	145	175	160	170	111	244	491	–
FM1 (1937-62)	MNHN	Femora	–	360	88.45	272	73.23	–	–	150	160	80	272	638	–
2014/0238/0049	NHMW	Tarsometatarsus	Juvenile	–	31	79	19	–	–	–	–	–	–	–	–
2014/0238/0048	NHMW	Tarsometatarsus	Juvenile	–	28	70	15	–	–	–	60	27	–	–	–
2014/0238/0036	NHMW	Tarsometatarsus	–	–	63	–	35	121	77	–	–	–	–	–	–
2014/0238/0034	NHMW	Tarsometatarsus	–	–	53	132	27	–	–	–	118	63	–	–	–
2014/0238/0033	NHMW	Tarsometatarsus	–	–	57	< 145	31	126	68	–	–	–	–	–	–
TMT2	MNHN	Tarsometatarsus	–	430	83	210	48	160	70	–	155	70	–	–	–
TMT1 (1906-16 Mr Belo)	MNHN	Tarsometatarsus	–	–	–	180	75	160	–	–	–	–	–	–	–
2014/0238/0051	NHMW	Fibula	–	–	26	–	19	30	60	–	–	–	–	–	–
2014/0238/0050	NHMW	Fibula	–	–	22	–	17	24	59	–	–	–	–	–	–

All the material from the NHMW was recovered from the Antsirabe. We are uncertain of the origin of the specimens from the MNHN.
Abbreviations: BM, body mass; Cr-Cd, craniocaudal; NHMW, Naturhistorisches Museum Wien, in Vienna, Austria; MHHW, Muséum National d'Histoire Naturelle in Paris, France.

Body mass estimation

The body mass of our aepyornithid specimens was calculated using the formulae of Campbell & Marcus (1992), which use the minimal circumferences of the femora and tibiotarsi (Table 1).

Sampling and pretreatment of bones for histological analyses

As far as possible, we sampled complete mid-diaphyseal cross-sections of the skeletal elements, but in a few cases (see Table 1) cores were taken from the bones using a 1 cm drilling core bit using the methodology outlined by Stein & Sander (2009). In cases where the cross-section of the diaphysis was too large to fit onto a 75 mm × 55 mm glass side, two glass slides were used to obtain composite transverse sections.

Assuming that some soft tissue remained in the sub-fossil material, all elements obtained from the NHMW were dehydrated preliminarily in three successive baths of 95% ethanol (with each lasting a minimum of 8 h), then defatted in two overnight baths of acetone. After the acetone treatment, the bones were left to dry completely before they were embedded in epoxy resin. The material from the MNHN was embedded in epoxy resin without pretreatment. Thin sections were prepared following the methodology outlined by Chinsamy & Raath (1992).

The terminology used here follows the traditional bone histology terminology *sensu* Francillon-Vieillot *et al.* (1990) and Chinsamy-Turan (2005). Note also that in general, the orientation and extent of the canals in the cortex are used as a proxy to describe bone vascularization, hence relative bone growth rates. However, each canal can house a variable number of blood vessels, in addition to nerves and connective tissues. Moreover, the orientation of the canals in the bone is not a direct reflection of the orientation of the blood vessels (Starck & Chinsamy, 2002; Chinsamy-Turan, 2005, 2012).

Thin sections were studied, and micrographs were taken using a Nikon E200 and a Zeiss petrographic microscope at the University of Cape Town (UCT), South Africa. For low-magnification images, we used an Olympus VS 120 virtual microscope scanner at UCT.

RESULTS

Our observations revealed that, in general, the bone histology of our specimens was well preserved. However, we found that the thin sections of the untreated MNHN material were a bit problematic because within a few hours of thin sectioning, the glass slide would fracture. We did not encounter such problems with the pretreated NHMW material; therefore, a pretreatment of sub-fossil material (as outlined above) is strongly recommended, before embedding and thin sectioning.

Using the equations of Campbell & Marcus (1992), we deduced that our sample represented individuals ranging in body mass from 83 kg, based on the smallest tibiotarsus (NHMW 2014/0238/0015), to 638 kg, based on the largest femur (MNHN FM1; Table 1).

In the following subsections, we describe the histology of the various skeletal elements from smallest to largest according to the taxonomic identification.

Histology of the juvenile specimens (unidentifiable at the genus/species level)

The smallest femur (NHMW 2014/0238/0052; Table 1) shows a well-preserved bone wall that at its thickest level measures 2567 µm (from the periosteal bone surface to the edge of the medullary cavity; Fig. 1A). The compacta is distinctly stratified into two types of bone tissues: an inner layer that opens into the medullary cavity and an outer layer that extends to the periosteal surface. These layers are distinctly separated by a line of arrested growth (LAG; Fig. 1B). The inner layer, which formed earlier in ontogeny is more compacted; it comprises of a fibrolamellar bone tissue with a predominance of reticular to longitudinal channels. This inner band of tissue is narrower, than the outer band, but this is a result of the expansion of the medullary cavity (Fig. 1B). The more recently deposited bone in the cortex is laminar FLB with a preferential circumferential orientation of the channels, although several canals in the cortex have a longitudinal arrangement (Fig. 1B). Osteonal development in the outer layer is incomplete, and several large open canals are evident within the scaffold of woven bone tissue. The outer margin of the bone is uneven and is clearly osteogenic (Fig. 1B).

A partial cross-section of the tibiotarsus of one of the juvenile specimens in our sample (specimen NHMW 2014/0238/0015) has a bone wall consisting of a narrow band of compacted bone tissue (Fig. 1C). The outermost (most recently formed) cortex is essentially formed of FLB with many circumferentially and longitudinally oriented primary osteons (Fig. 1C, D). The peripheral margin of the bone is uneven, pierced by vascular canals, and appears to be in a state of active osteogenesis (Fig. 1D, E). In the mid-cortical region, there are two growth marks (narrow annuli) visible in parts of the compacta (Fig. 1D). Internal to the inner growth mark are many secondary osteons (Fig. 1D). Many of these are completely formed secondary osteons, but a few enlarged cavities are still evident (Fig. 1C, D). Below this region, the bone appears to be fractured, and several thin, 'loose' trabeculae are evident in the

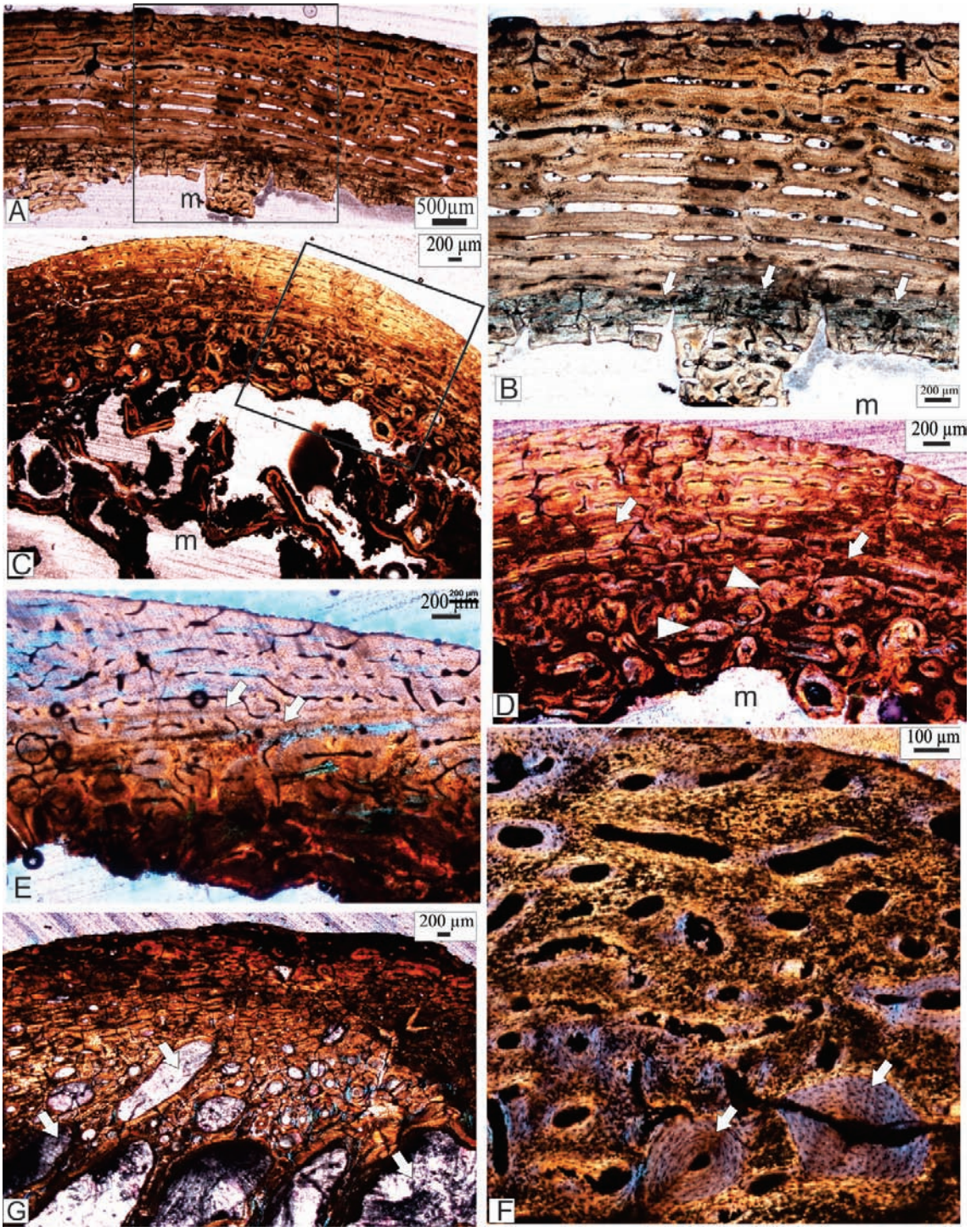

Figure 1. A, B, femur, NHMW 2014/0238/0052, transverse section. A, a low-magnification image of the overall histology of the bone wall. Abbreviation: m, medullary cavity. B, higher magnification of the boxed part of the cortex in panel A, showing the inner and outer layers of bone tissue separated by a line of arrested growth (white arrows). Note that the inner layer, closest to the medullary cavity (m), comprises reticular fibrolamellar bone, whereas the outermost layer consists of more laminar bone tissue. C–G, tibiotarsus NHMW 2014/0238/0015, transverse section. C, low magnification, giving an overall view of the bone wall. Abbreviation: m, medullary cavity. D, higher magnification of the boxed region in panel C, showing the highly secondary reconstructed inner part of the bone wall, with many secondary osteons (arrowheads), and

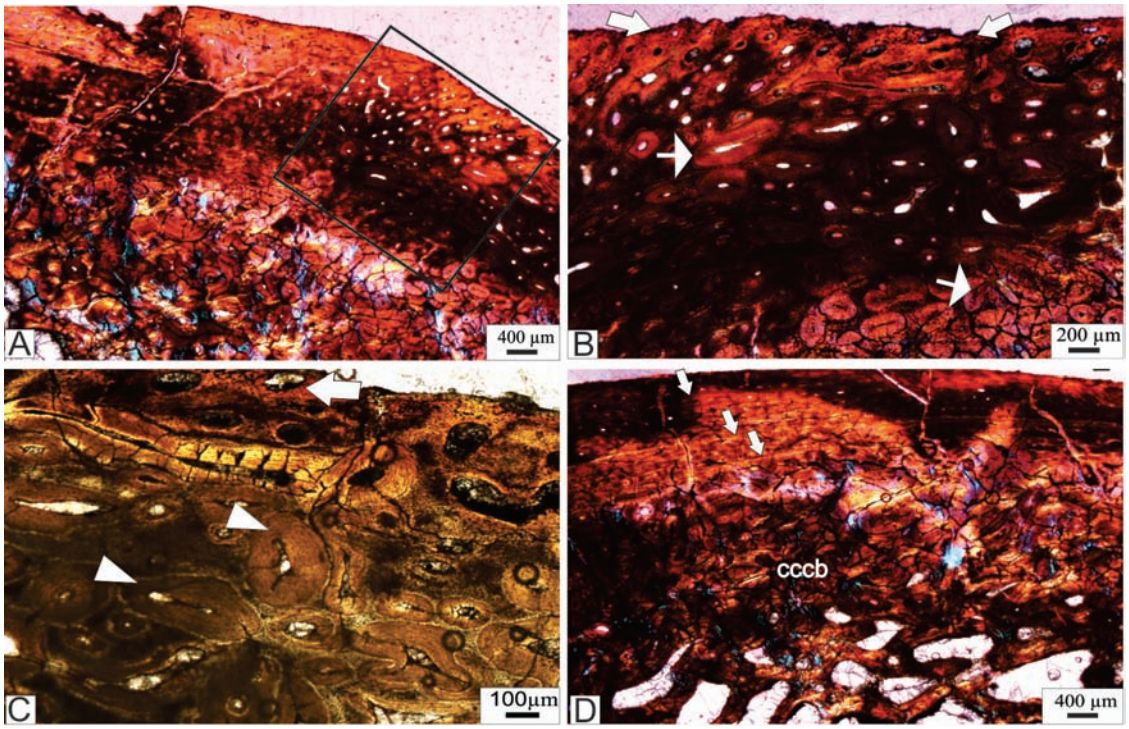

Figure 2. Tibiotarsus NHMW 2014/0238/0009, transverse section. A, low magnification, showing an overall view of the histology of the thick bone wall. B, higher magnification of the lateral edge of the cortex indicated by the box in panel A, showing the uneven osteogenic peripheral margin (outer arrows) and the formation of primary osteons in the peripheral region, in addition to the extensive development of secondary osteons in the cortex (inner arrows). C, higher magnification, showing the early stages of primary osteon formation (arrow) and the well-developed secondary osteons deeper in the cortex (arrowheads). D, posterior part of the cortex, showing the periosteal bone tissue interrupted by three lines of arrested growth (arrows), in addition to the extensive development of compact coarse cancellous bone (cccb), which is followed by a region with several enlarged resorption cavities.

medullary cavity (Fig. 1C). A thin section of a different part of the shaft shows that the bone wall essentially consists of FLB. Two growth marks (narrow annuli) are also evident in the cortex (Fig. 1E), immediately above the zone of secondary reconstruction of the earlier formed bone. Secondary osteons are also scattered in some parts of the outermost cortex (e.g. Fig. 1F). In a different bone fragment of the shaft, extensive secondary reconstruction extends right to the edge of the peripheral margin (Fig. 1G), and several large erosion spaces occur, with some of them enlarged to reach cancellous dimensions and extending into the medullary cavity (Fig. 1G).

Tibiotaral specimen NHMW 2014/0238/0009, although slightly larger, is also a juvenile specimen (Table 1). Fibrolamellar bone with many circumferentially and longitudinally oriented canals are the predominant tissue in the cortex, although other types of bone tissues are also present. For example, the lateral edge of the cortex shows an uneven texture and appears to be a region where the deposition of FLB with longitudinally oriented canals was underway (Fig. 2A, B). Directly preceding this outer region is a zone comprising well-formed secondary osteons (Fig. 2C), which merges with a region of compacted coarse cancellous bone (cccb; Fig. 2A, D). In the posterior part of the compacta, > 50% of the bone wall consists of cccb (Fig. 2D). At least three narrow annuli interrupt the deposition of fibrolamellar bone in the outermost cortex, and the perimedullary tissue in this region has a more spongy texture (Fig. 2D).

the outer region, with largely unremodelled fibrolamellar bone tissue interrupted by growth rings (arrows). E–G, different transverse sections of bone fragments of the tibiotarsus. E, the reticular fibrolamellar bone tissue interrupted by two narrow annuli (arrows). F, higher magnification, showing the fibrolamellar bone and a few secondary osteons (arrows). G, transverse section of a different shaft fragment, showing a more extensively remodelled cortex. Several large resorption cavities (arrows) are visible.

The histology of two juvenile tarsometatarsi was studied (NHMW 2014/0238/0049 and NHMW 2014/0238/0048; Table 1). The former specimen is the smallest in our sample and preserves most of its cross-sectional bone wall. The anterior part of the cortex consists of many longitudinal primary osteons within a woven fibred bone matrix (Fig. 3A), although several large erosion cavities are clearly visible in the compacta. The peripheral margin is uneven, and it is apparent that growth in diameter with periosteal bone deposition was underway here. The perimedullary margin is clearly resorptive. Tiny bits of plant matter, including a piece of a root, are present within the medullary cavity (Fig. 3A, B).

The medial part of the shaft is thickest, with the outermost bone wall consisting of longitudinally oriented primary osteons, followed by cccb and then large cancellous spaces that extend into the medullary cavity (Fig. 3C). The posterior part of the bone wall appears to be the narrowest and shows some primary bone but is extensively reconstructed in the deep cortex (Fig. 3D). Overall, the cross-section of the bone has a rather spongious aspect, and the peripheral edge is clearly uneven and appears to have been active in osteogenesis (Fig. 3B). Towards the medullary cavity, large erosion cavities are present, several of which reach cancellous proportions (e.g. Fig. 3A, C).

The next smallest tarsometatarsus in the sample (specimen NHMW 2014/0238/0048; Table 1) has a thick cortex, largely made up of compact reticular FLB bone (Fig. 4A, B). Near the periphery, newly formed bone tissue is visible, and periosteal bone deposition was underway at the time of death (Fig. 4A, B). Towards the medullary cavity, secondary reconstruction is extensive, and several secondary osteons are present, in addition to several enlarged canals (Fig.4A, B). Some of these coalesce to form large vacuities within the bone wall. The cores of the bony struts that extend into the medullary cavity contain remnants of the deep cortical tissue and are sometimes lined with endosteally formed lamellar bone (Fig. 4A, C). In sections taken towards the distal metaphysis, the struts extend right across the medullary cavity.

Histology of the *A. hildebrandti* specimens

The smallest *A. hildebrandti* femur (NHMW 2014/0238/0038; Table 1) in our sample belongs to an individual that has more than doubled in mass in comparison to our smallest aepyornithid specimen (Table 1). Unfortunately, the whole cortex of the cross-section is not preserved. Only part of the bone wall is visible and consists of FLB tissue with a large number of longitudinal primary osteons towards the periphery, with secondary osteons towards the endosteal region, and a single growth mark (LAG) is visible towards the outer part of the cortex (Fig. 4D, E). In parts where the outermost region is preserved, this is uneven and appears resorptive. Most of the vascular canals are primary osteons, but some secondary osteons are also evident in the compacta. Several enlarged erosion bays are present, which indicate that a considerable amount of remodelling has occurred, and thin struts of bone extend into the expanding medullary cavity (Fig. 4D).

Two tarsometatarsi specimens of *A. hildebrandti* were studied: NHMW 2014/0238/0034 and NHMW 2014/0238/0036. The latter sample shows some diagenetic alteration, but it is evident that the compacta is highly remodelled and that there are a large number of erosion cavities near the medullary cavity. Specimen NHMW 2014/0238/0034 is much better preserved and shows predominantly an extensively reconstructed compacta, with limited amounts of primary bone tissue evident in the bone wall (Fig. 4F), although the tissue does not reach dense Haversian levels. Enlarged cavities are evident near the medullary cavity (Fig. 4F), and there are several bony struts that extend across the medullary cavity.

Histology of the *A. maximus* specimens

Two large femora (MNHN specimens FM3 and FM2) in our sample have maximum lengths of 35 and 38 cm, respectively (Table 1), with an estimated mass of 491 kg for both individuals. The bone wall of FM3 is composed of predominantly primary bone tissue, although many large erosion spaces occur in the perimedullary region, and sometimes these merge to form large cancellous areas and bony struts that extend into the medullary cavity (Fig. 5A). The anterior and posterior parts of the bone wall are thickest and measure ~9 mm. However, if we consider the struts of the primary bone as indicative of the total cortical bone deposited through ontogeny, it is estimated that this would have been ~27 mm (in the anterior region). The FLB tissue presents a preferential laminar organization of the vascular canals in some parts (Fig. 5B) and reticular in other parts (Fig. 5C). Additionally, several large radial canals extend across the compacta. Primary osteons are evident right up to the peripheral edge of the bone wall, suggesting that growth is ongoing. Growth marks are scarce, with only one or two possible LAGs visible in the cortex, but they generally cannot be followed completely around the cross-section. Isolated secondary osteons are sparse in the compacta.

Specimen FM2 represents the longest femur in our sample (Table 1) and preserves a thick, compact bone wall (Fig. 6A). About seven LAGs are distinctive in the outer third of the compacta (Fig. 6B). This outermost region of the cortex also shows a dramatic decrease in vascularization and a change to a more parallel-fibered to lamellar bone tissue, which is indicative of

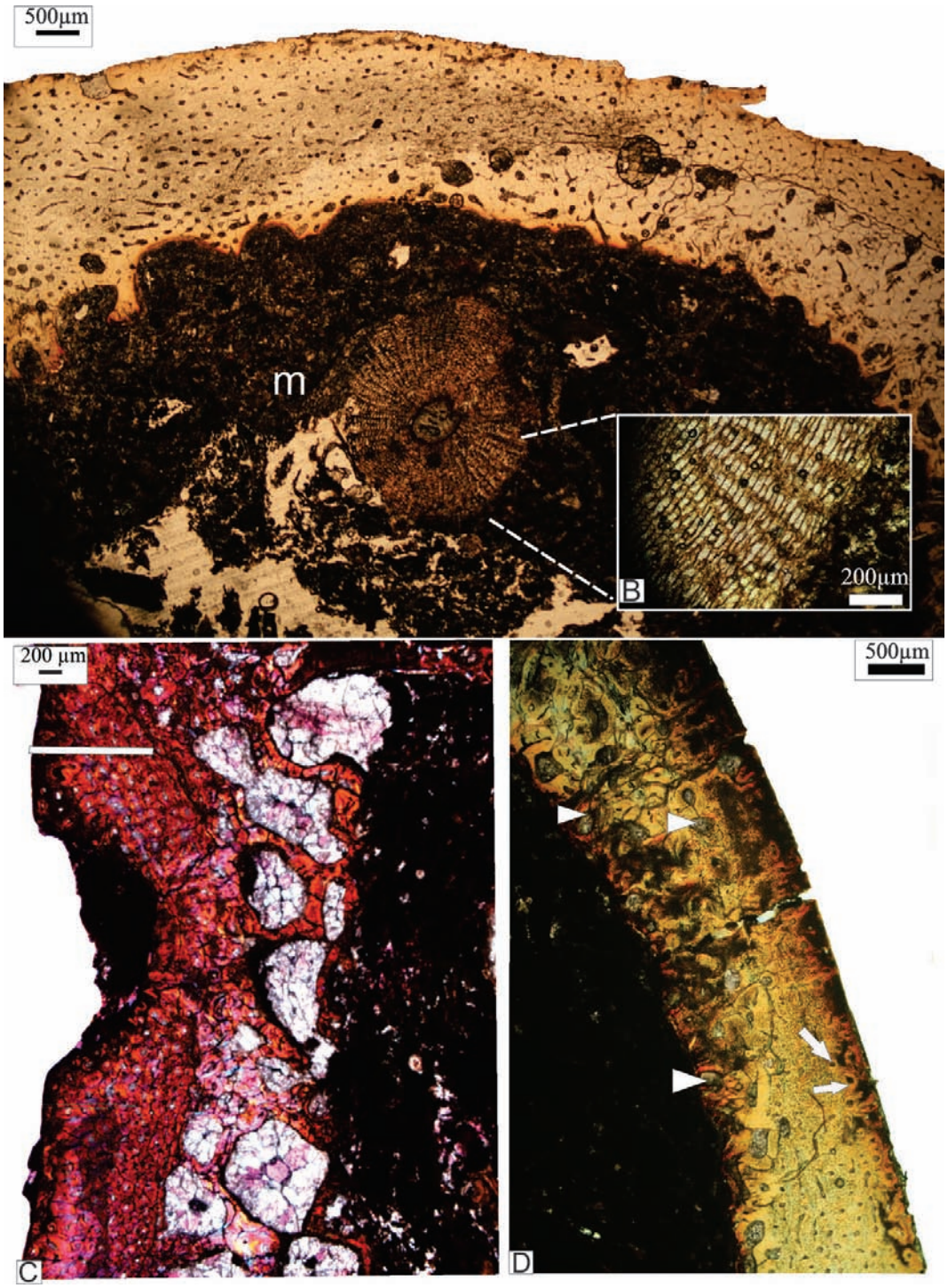

Figure 3. Tarsometatarsus, NHMW 2014/0238/0049, transverse section. A, anterior part of the bone wall, showing a richly vascularized cortex. Several enlarged resorption cavities are evident in the cortex, and the endosteal margin of the bone is clearly resorptive. The peripheral region appears to be osteogenic. Within the medullary cavity (m) lies a circular structure that appears to be a section of a root. B, high magnification of the root section, showing details of the cellular structure. C, transverse section of the medial part of the bone wall, showing primary bone tissue in the outermost periphery (white bar), below which is a region of compact coarse cancellous bone, followed by a region of cancellous bone tissue. D, posterior part of the bone wall, showing a heavily remodelled cortex, with several completely formed secondary osteons (arrows), and many enlarged erosion cavities (arrowheads), with secondary deposits of lamellar bone.

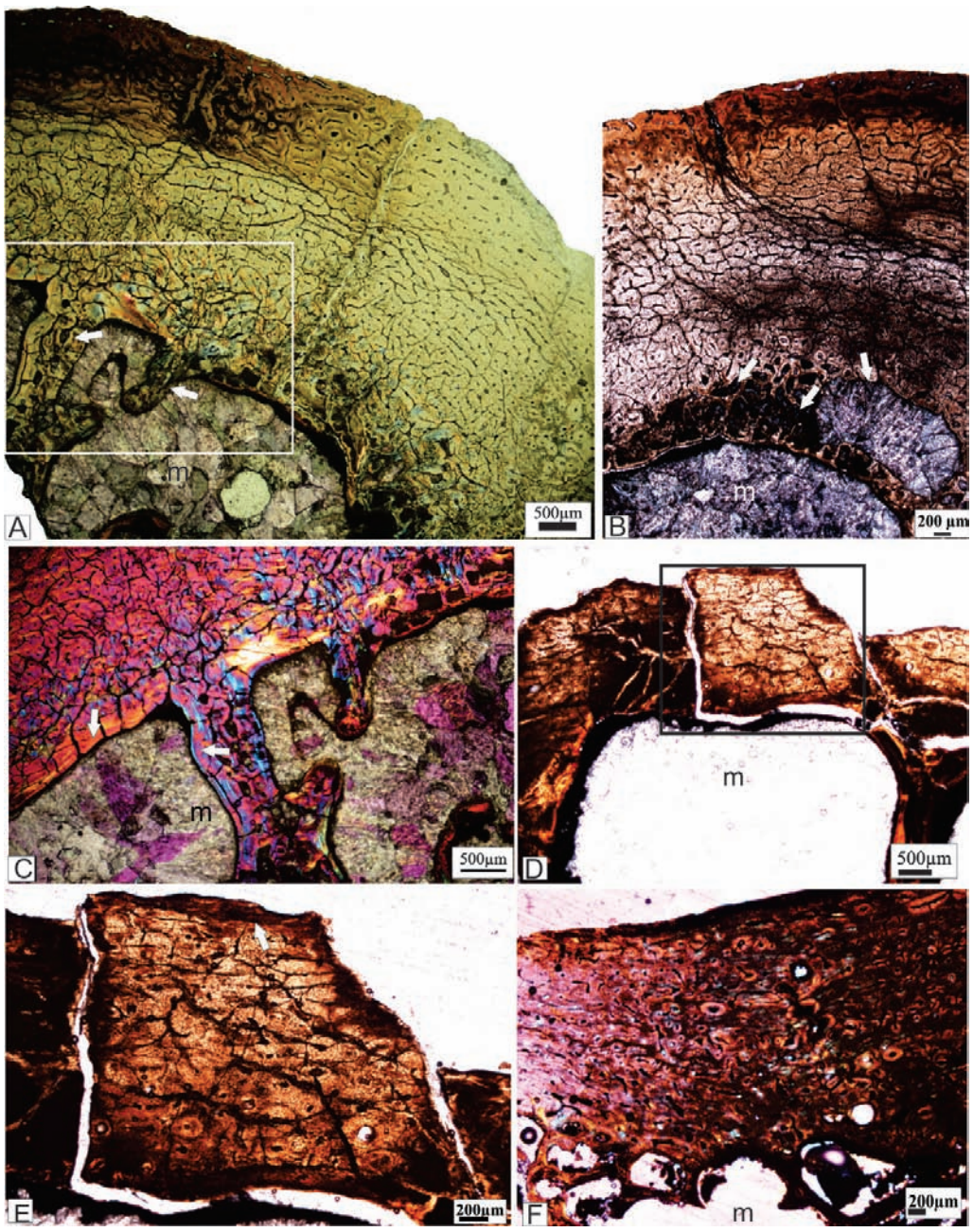

Figure 4. Tarsometatarsus, NHMW 2014/0238/0048, transverse section. A, overview of the thick bone wall surrounding the medullary cavity. The outermost margin of the bone appears to be uneven and osteogenic. The innermost region appears to be heavily reconstructed, and trabeculae (arrows) extend into the medullary cavity (m). B, higher magnification of a different part of the bone wall, showing that the outermost peripheral region is still forming bone, followed by a region of primary reticular bone tissue overlying a region of secondary reconstructed bone tissue. Nearest the medullary cavity (m) are several enlarged resorption cavities (arrows), some of which coalesce to form a cancellous textured bone tissue. C, higher magnification of the region indicated by the box in panel A, showing the innermost part of the cortex and the trabeculae that extend into the medullary cavity. Note the narrow lamellar bone deposits (arrows) that line the trabeculae and medullary cavity (m). D, transverse section of femur NHMW 2014/0238/0038, showing the narrow compact bone wall and a large amount of remodelling in the endosteal region. Abbreviation: m, medullary cavity. E, higher magnification of the boxed region in panel D. F, tarsometatarsal NHMW 2014/0034, showing the highly secondary reconstructed cortex.

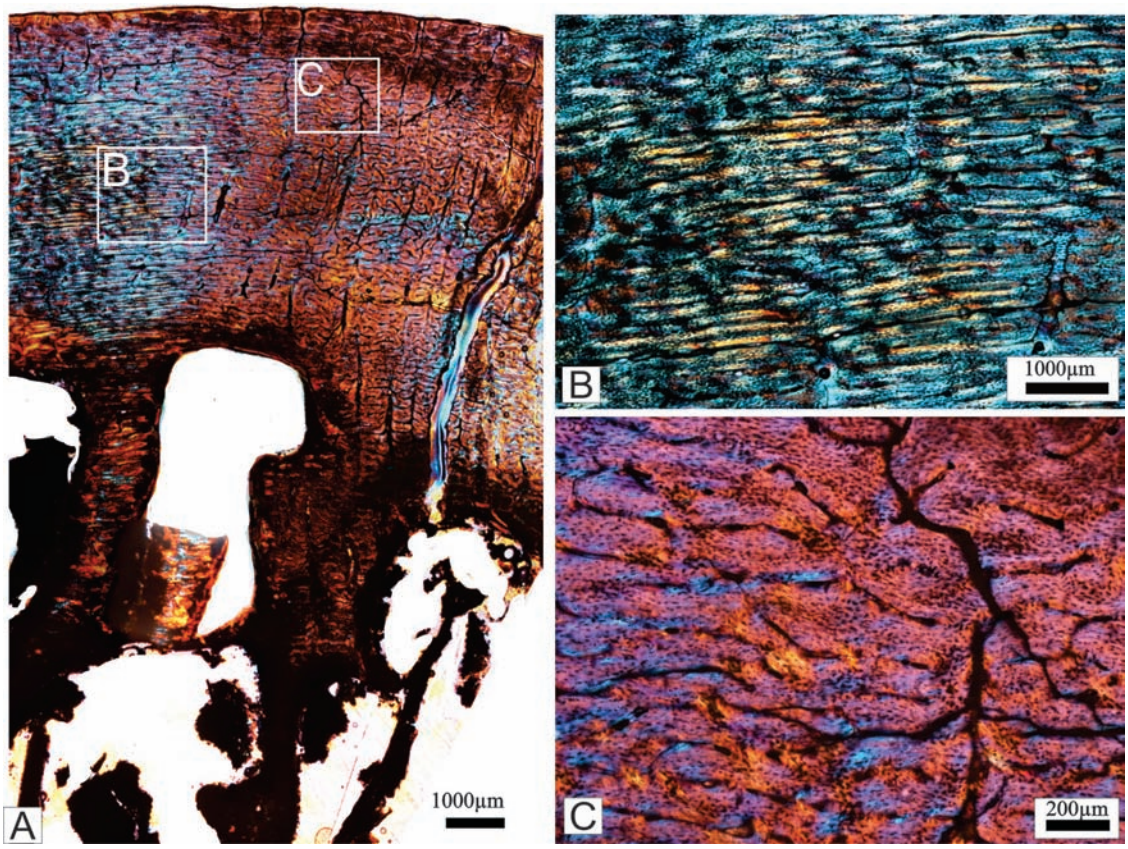

Figure 5. Femur, MNHN FM3, of *Aepyornis maximus*, transverse section. A, low magnification, showing an overall view of the bone wall. Note the predominantly primary nature of the outer part of the compacta and the large radial canals that traverse the cortex. The internal areas of the compacta are extensively remodelled. B, higher magnification of the larger boxed region in panel A, showing the laminar nature of the bone tissue. C, higher magnification of the smaller boxed region in panel A, showing the reticular nature of the bone tissue and details of the large radial canals that connect multiple vascular canals.

bone deposition slowing down (Fig. 6B). Internal to this tissue is fibrolamellar bone tissue, with a high density of small and primarily circumferential vascular canals associated with some large radial canals running perpendicular to the successive vascular laminae. Patches of Sharpey's fibres are also evident in the tissue of this region. Towards the outer cortex, the annuli are also more closely spaced (Fig. 6B). The outer two-thirds of the bone wall consist essentially of primary periosteal bone tissue, whereas the inner one-third shows extensive secondary remodelling, with several large erosion cavities (Fig. 6A). The innermost region shows thick layers of endosteally formed lamellar deposits that line large cancellous spaces (Fig. 6C, E). The lamellar bone within these spaces often has hypermineralized lines, indicating successive resorption–redeposition cycles (Fig. 6C, E). Interestingly, the orientation of some osteocytes in these lamellar deposits is variable and sometimes perpendicular to the lamellae (Fig. 6D). Within some of these large cancellous spaces, there are deposits of woven bone tissue, with many globular osteocyte lacunae and some simple blood vessels (Fig. 6A, E, F). This unusual tissue appears to develop within closed vacant spaces in the sub-endosteal region of the cortex; it forms neither along the endosteal margin nor along the struts of trabecular bone. In some areas, this tissue shows evidence of resorption (Fig. 6A, E). As in FM3, secondary osteons are sparse in the compacta.

Tibiotarsal specimen NHMW 2014/0238/0021 preserves only part of the bone wall, and there are significant regional changes in the bone microstructure. For example, there is a distinctive change from mainly primary bone tissue along the posterior–lateral side of the bone wall (Fig. 7A) to a predominantly secondary compacta on the anterior part of the bone wall. In this region, secondary reconstruction has progressed substantially, meaning that now many more secondary osteons are scattered in the cortex (although they never reach dense Haversian proportions; Fig. 7B,

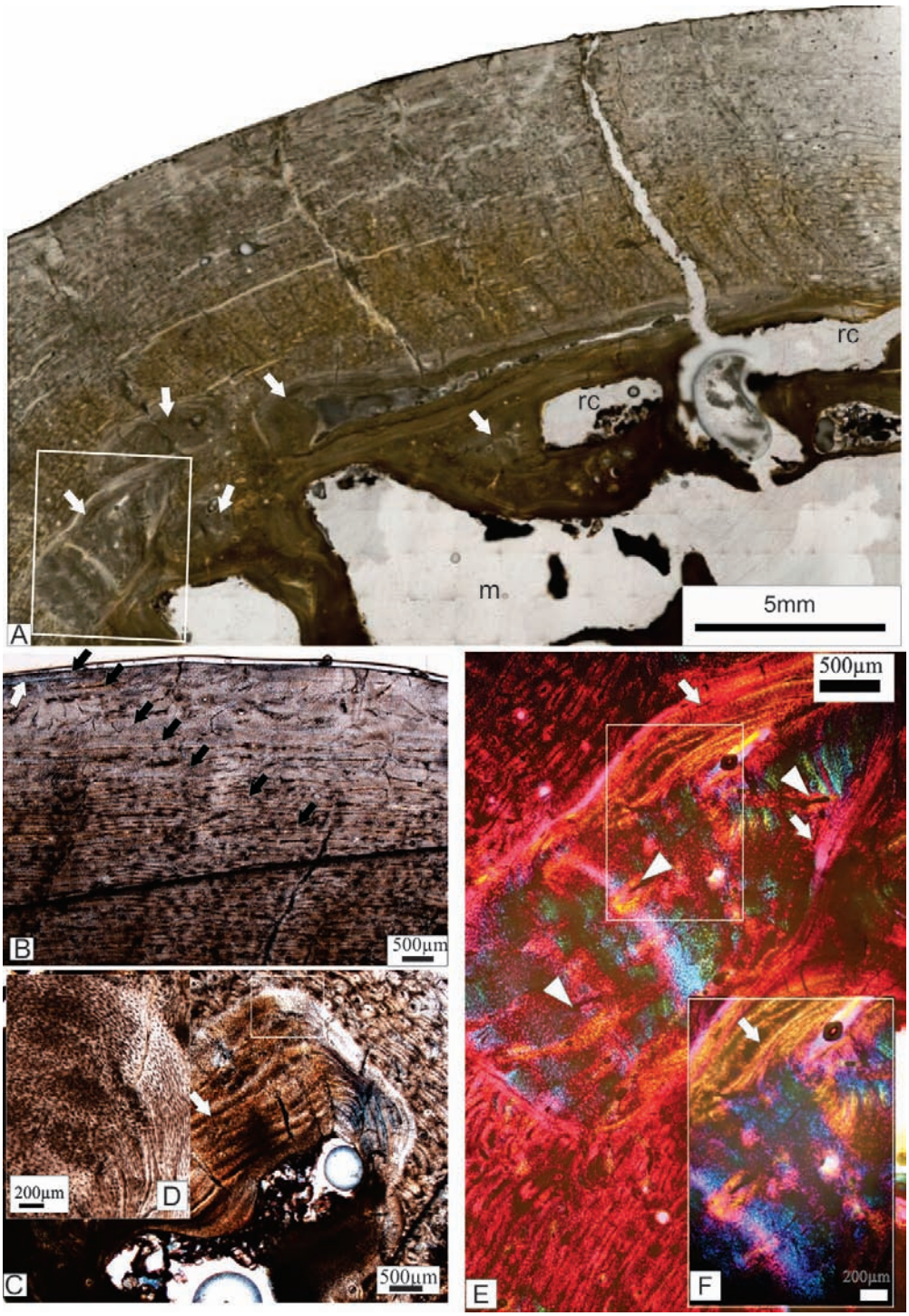

Figure 6. Femur, MNHN FM2, of *A. maximus* transverse section. A, a low-magnification image of the bone wall, showing the extensive bone remodelling in the perimedullary region. Several large resorption cavities (rc) are evident. Some of the large resorption spaces in the subendosteal region show a secondary infillings (arrows) of bone tissue. Abbreviation: m, medullary cavity. B, higher magnification, showing the fibrolamellar bone tissue interrupted by several growth rings (black arrows). The white arrow points to the outer circumferential layer. C, higher magnification of an erosion cavity, showing several episodic cycles of deposition of lamellar bone (arrow). D, higher magnification of the boxed region in panel C, showing the different orientations of the osteocyte lacunae. E, higher magnification of the boxed region in panel A, showing the histological detail of the secondarily deposited endosteal lamellar bone tissue (arrows) and the woven bone with simple

C). The secondary osteons often interrupt the growth rings (which tend to be narrow annuli with or without LAGs) and sometimes completely obliterate them, although in several places in the cortex growth marks are still observed (Figs. 7C, D). Particularly large erosion cavities are present in the perimedullary region (Fig. 7A). The lateral part of the bone wall has less secondary reconstruction in the outer part of the compacta, which is still mainly a plexiform type of FLB tissue. However, about two-thirds into the compacta large erosion cavities occur, and they become increasingly larger towards the perimedullary region and finally result in a large number of trabecular struts that extend into the medullary cavity (Fig. 7A).

A single tarsometatarsus of *A. maximus* (NHMW 2014/0238/0033) was examined histologically. The histology of the section is not well preserved, because many microcracks disrupt the bone tissue, but it is nevertheless evident that the compacta is highly remodelled, and there are secondary osteons present right up to the peripheral margin of the bone.

Histology of the *V. titan* specimens

Although FM1 is not the longest femur, its relative circumference is larger than the two *A. maximus* femora, and the mass of the associated individual is estimated as 638 kg. The cortex consists of FLB with a mixture of plexiform/laminar and reticular organized vascular canals (Fig. 8A), and there is a distinct annulus visible in the compacta (Fig. 8B). The bone walls are composed of predominantly primary periosteally formed bone tissue, although secondary osteons are scattered throughout the compacta and some are found close to the periphery (Fig. 8A). Reticular FLB occurs at the periphery, indicating that bone formation was still rapid in this large individual (Fig. 8B). Large erosion bays are present towards the perimedullary region.

Specimen MNHN TMT1 is the largest tarsometatarsus of all our Aepyornithidae specimens. It has a thick cortex that consists of a large amount of secondary reconstruction, which is extensive near the medullary cavity, reaching dense Haversian proportions. Towards the periphery, there is still a large amount of secondary reconstruction underway, but nearer the edge of the bone surface large amounts of primary reticular fibrolamellar bone tissue are still present (Fig. 8C).

The dimensions of tibiotarsal specimen TB6 (MNHN) suggest that it belonged to a large individual (Table 1). The thin section shows that the outermost cortex appears to be primary reticular FLB with at least one narrow annulus (Fig. 9A). Overall, the texture of the bone and more sparsely distributed vascular canals suggests that the rate of bone deposition has reduced. Several completely formed secondary osteons are evident throughout the cortex, and inner areas of the bone are more highly remodelled. The innermost margin of the bone is highly resorptive, and no trabeculae are visible.

Specimen TB5 (MNHN) is one of the largest tibiotarsal specimens in our sample. The cortex is highly remodelled, but several growth cycles are still evident (Fig. 9B). Secondary osteons occur right up to the peripheral margin of the bone wall. Towards the medullary cavity, some larger erosion rooms reach cancellous dimensions and have narrow deposits of endosteal lamellar bone (Fig. 9C).

Tibiotarsal specimen TB1 (MNHN) (Table 1) shows extensive secondary reconstruction right up to the peripheral edge of the bone wall (Fig. 9D). Secondary osteons are dense in the mid-cortical to perimedullary regions, with some evidence of overlapping generations of secondary osteons, but they do not reach dense Haversian bone proportions (Fig. 9D, E).

Histology of the unidentifiable adult aepyornithid specimens

The femur (specimen NHMW 2014/0238/0046; Table 1) shows variable thickness of the bone wall in different parts of the cross-section. The posterior part of the bone wall is extensively remodelled, with imbalance towards resorption, such that only a thin portion of the cortex remains (Fig. 10A). The medial to anterior part of the bone wall is thickest. At least four growth cycles are evident in the compacta, and the widths between them appear to be decreasing towards the periphery (Fig. 10B). These consist of narrow lamellar deposits (annuli) that alternate with a densely vascularized laminar FLB bone tissue traversed by large radial connections (Fig. 10A, B). Large erosion cavities traverse the primary compacta, and occasional struts of primary bone protrude into the medullary cavity (Fig. 10A, B).

The cortex of the femur NHMW 2014/0238/0047 (Table 1) shows a thick bone wall consisting of plexiform FLB and a large number of secondary osteons present in the compacta (Fig. 10C). At least two or three narrowly spaced annuli are evident in the peripheral region of the compacta. It is uncertain how many earlier cycles might have been eroded by secondary reconstruction, because several large erosion cavities

vascular canals (arrowheads) that infilled the resorption cavity secondarily. F, higher magnification of the boxed region in panel E, showing the woven texture of the infilling bone. Arrow indicates part of the outer lamellar lining of the cavity.

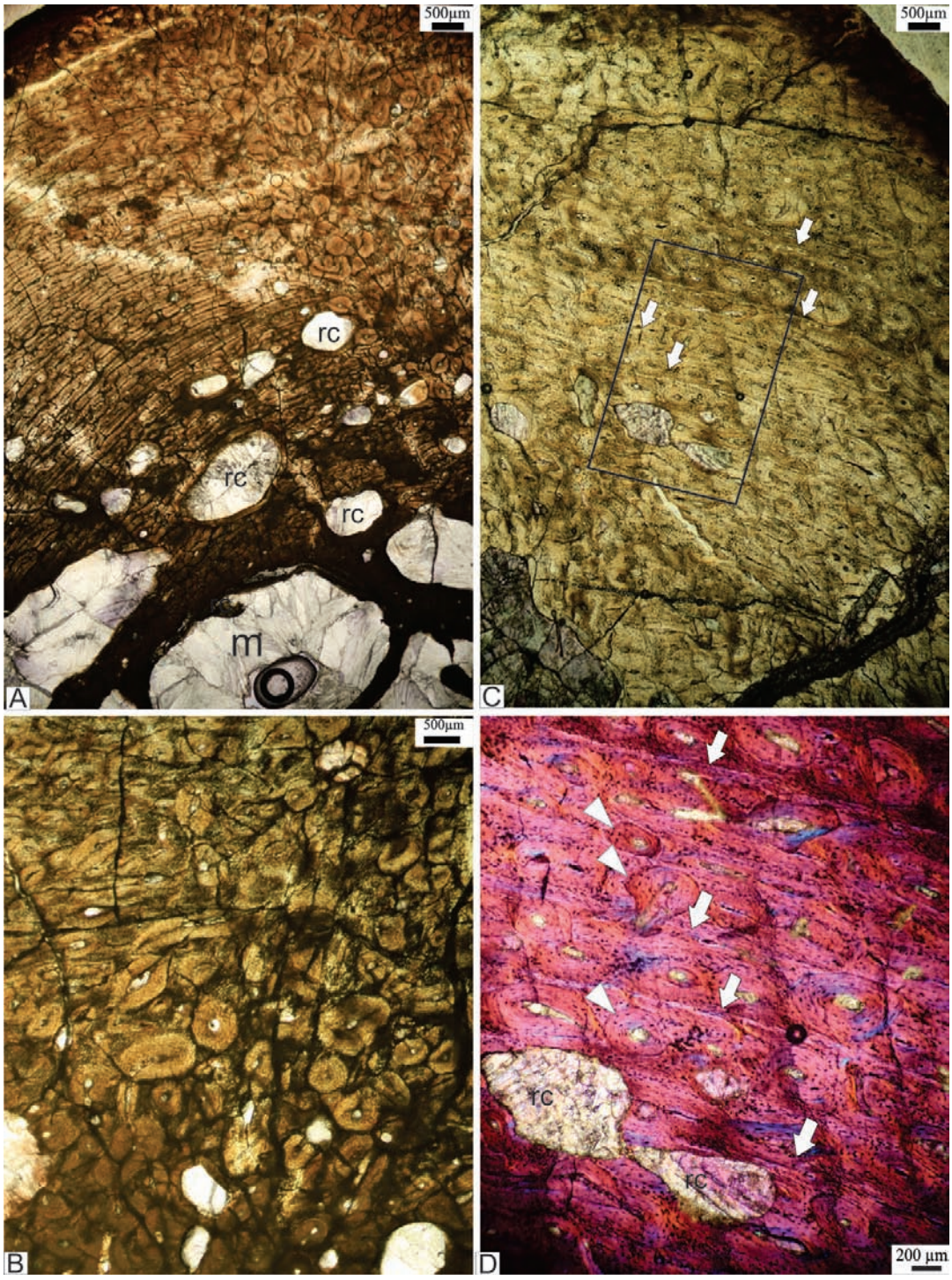

Figure 7. Tibiotarsus, NHMW 2014/0238/0021, transverse section. A, the lateral part of the bone wall is on the left of the image and shows the largely primary cortex, with some scattered intracortical remodelling evident. Notice the many resorption cavities (rc) visible and their increasing size towards the medullary cavity (m). Towards the right is the anterior part of the bone wall, which exhibits distinctly more extensive remodelling throughout the cortex. B, higher magnification of this region. C, section showing an anterior part of the bone wall, with more secondary reconstruction evident throughout the cortex. Note that several growth rings are still visible despite the intracortical remodelling. D, higher magnification of the boxed region in panel C, showing the resorption cavities (rc) and several completely formed secondary osteons (arrowheads). Arrows indicate lines of arrested growth.

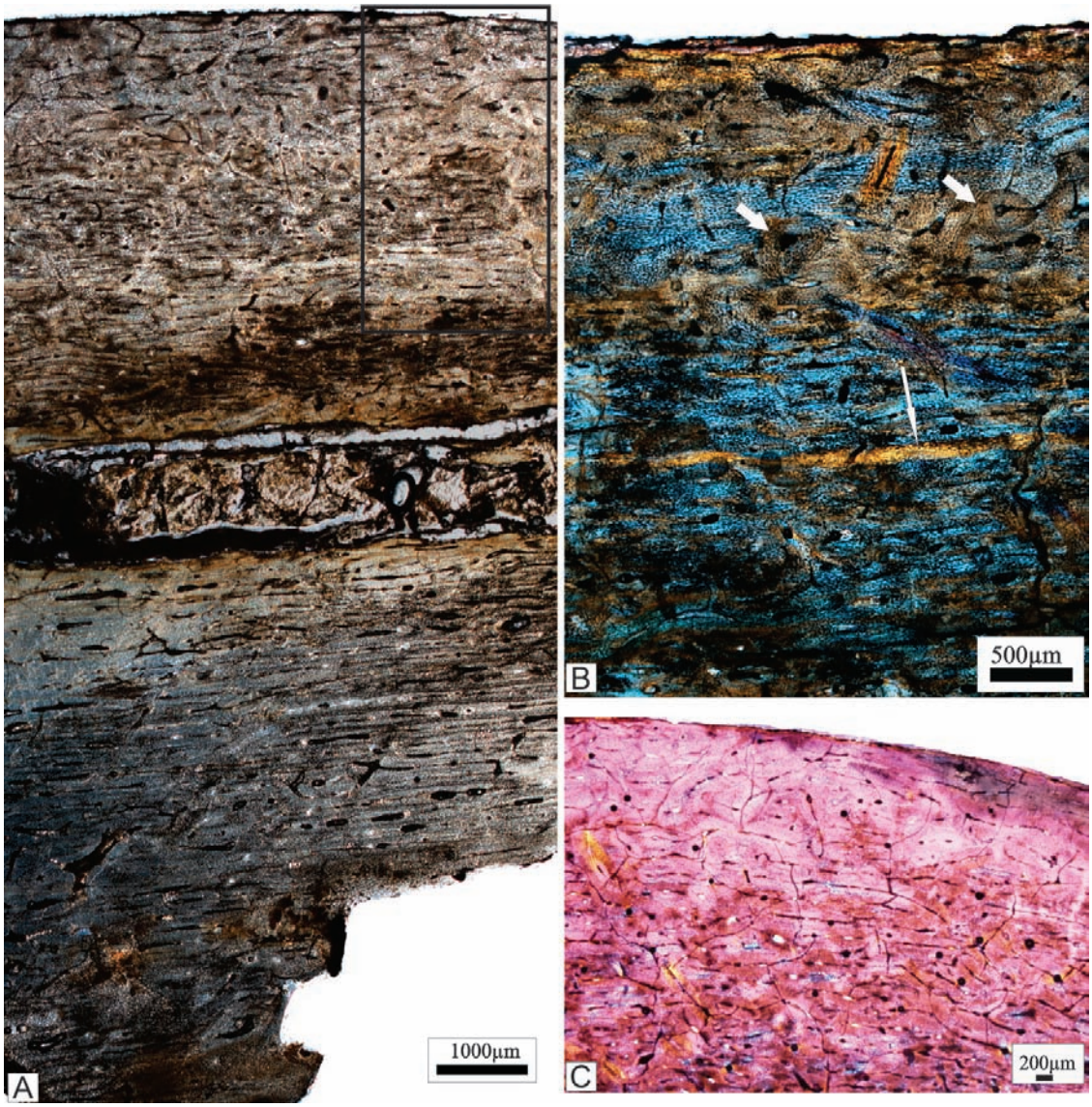

Figure 8. Core of femur, MNHN FM1. A, low magnification, showing the overall view of the compacta. B, higher magnification of the boxed region in panel A, showing histological details of the bone tissue. Note the few secondary osteons (arrows) located near the periphery and the narrow annulus (thin arrow). C, tarsometatarsal MNHN TMT1, showing largely primary reticular bone towards the periphery, although more internally there are increasingly more secondary osteons and enlarged resorption cavities present.

are evident in the cortex. These cavities are lined with a narrow deposit of endosteally formed lamellar bone tissue.

The tibiotarsal specimen NHMW 2014/0238/0017 has a thick bone wall, with several growth cycles evident in the compacta (Fig. 10D). The growth rings appear to be narrow bands of annuli consisting of lamellar tissue (Fig. 10E), which are not formed at regular intervals and, as such, there is a variable amount of FLB deposited in between them. The FLB tends to vary between reticular and laminar arrangements with radial anastomoses and, in general, there is a decrease in the amount of vascularization towards the outer cortex. Secondary osteons are not densely developed and appear scattered throughout the compacta (Fig. 10D, E). Although the entire bone wall is not preserved, it is apparent that there are some enlarged resorption cavities towards the medullary region, with many of them reaching cancellous proportions.

The histology of two fibulae, NHMW 2014/0238/0050 and NHMW 2014/0238/0051, was studied. The partial transverse section of fibula NHMW 2014/0238/0051

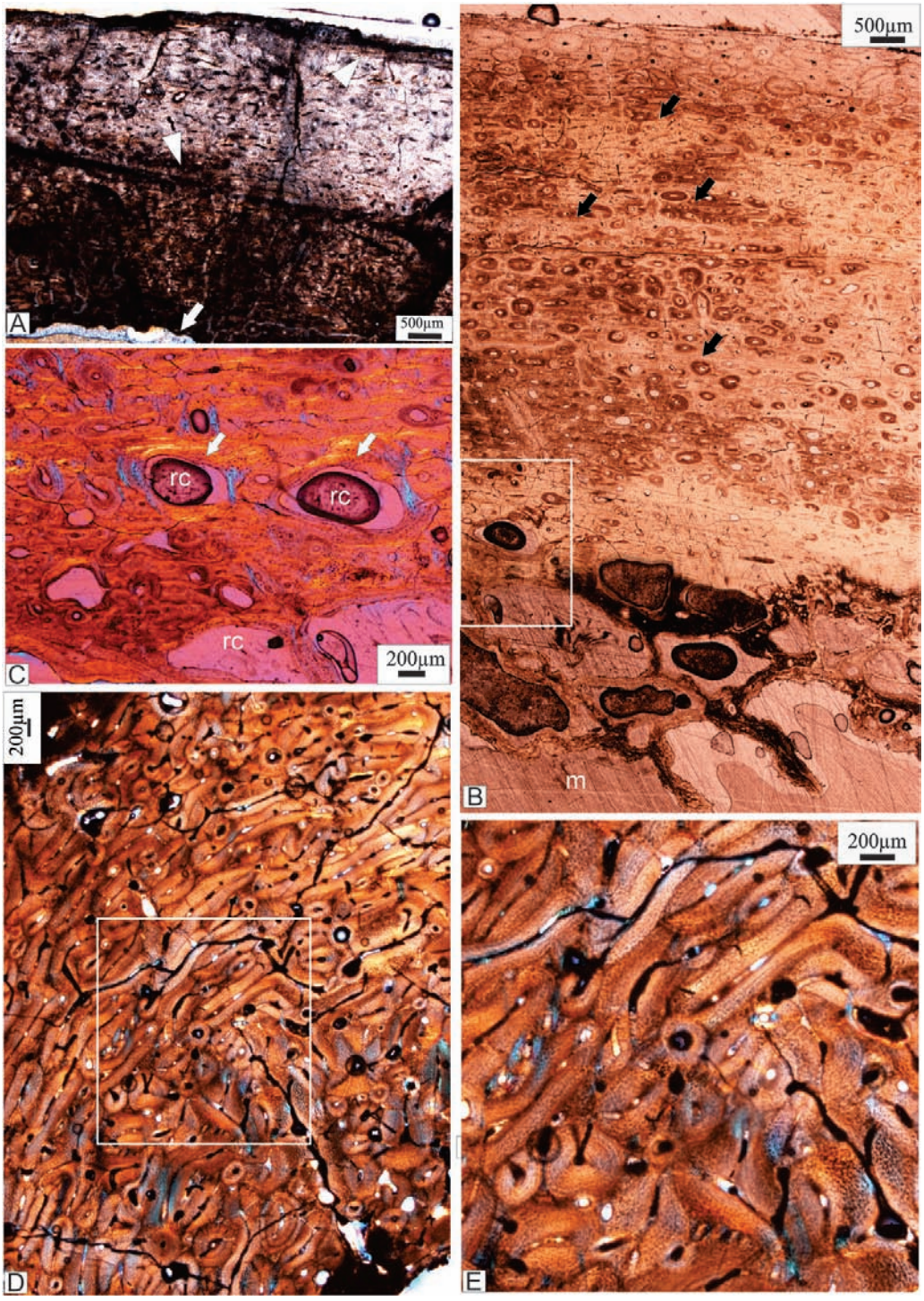

Figure 9. A, tibiotarsus TB6 (MNHN), transverse section. The section indicates that there has been substantial resorption (arrow) from the endosteal margin of the bone wall. The peripheral margin appears to be uneven and still forming bone. The external part of the compacta consists mainly of a reticular type of fibrolamellar bone tissue. One distinctive growth ring (arrowhead) is evident in the mid-cortex and, possibly, another immediately beneath the peripheral margin. B, tibiotarsus TB5 (MNHN), transverse section. Intracortical remodelling occurs throughout the cortex, although it is more heavily developed towards the medullary cavity (m). Despite the secondary reconstruction, several growth rings (arrows) are visible. C, higher magnification of the boxed region in panel B, showing several enlarged resorption cavities (rc). Many of these show centripetal deposits of lamellar bone (arrows). D, TB1 (MNHN), transverse section, showing the extensive

shows variable bone wall thickness across the section, with the lateral part of the bone wall having the thickest cortex (Fig. 11A). The lateral part of the bone wall consists of extensively reconstructed bone tissue that reaches dense Haversian proportions (Fig. 11B) from the peripheral margin right up to the inner cortex where the cancellous bone begins. The outermost bone tissue in the anteromedial part of the bone appears to be a narrow layer of lamellar bone tissue, beneath which occurs an area of heavily reconstructed bone tissue (Fig. 11C, D). Closer to the medullary region there appears to be a layer of primary bone tissue with scattered secondary osteons and Sharpey's fibres (Fig. 11F). Below this is an area of enlarged erosion cavities that extend into the medullary region, forming large cancellous spaces, some of which are lined by thin deposits of endosteally formed lamellar bone (Fig. 11C). Some of the struts of cancellous bone have secondary osteons (Fig. 11C). The anteromedial side of the bone wall has a much more reduced band of compact bone tissue and has a higher concentration of large cancellous spaces (Fig. 11F).

The other fibula (specimen NHMW 2014/0238/0050) preserves only part of the bone wall, and this region essentially consists of dense Haversian bone (Fig. 11G).

DISCUSSION

Bone histology of the hindlimb skeleton of aepyornithids revealed substantial variation that appeared to be related to ontogenetic age, the localized growth dynamics of the skeletal element, the biomechanical loading regimens experienced by the bone and possible taxonomic differences. Given that we had a limited number of elements from each taxon and that these were at different ontogenetic stages, we were unable to discern whether there was a taxon-specific histology. However, it appeared that the two *A. maximus* femora were similar in that they had predominantly primary cortex consisting of laminar FLB and large radial canals connecting multiple laminae, a feature not seen in the single core sample we had of *Vorombe*. Interestingly, such radial canals traversing large areas of the compacta have been observed in the tibia of modern giraffes (Caitlin Smith, personal communication, 2020). When similar sized femora of *A. maximus* and *V. titan* were compared, the former tended to have a predominantly primary compacta with scarce secondary reconstruction, whereas the latter was more heavily reconstructed (and showed Haversian tissue; see section below on Femoral histology of adult Aepyornithidae).

The juveniles clearly showed more rapidly formed bone tissue with large vascular spaces and uneven endosteal and periosteal margins indicative of remodelling (*sensu* Enlow, 1963). Interestingly, irrespective of taxonomic identity, our study showed that different bones of the hindlimb exhibited different types of histology, which suggested different rates of growth: the femora showed a preponderance of laminar fibrolamellar bone tissue (with many circumferentially oriented vascular canals and, in the case of *A. maximus* femora, large radial canals extending across the compacta and connecting the circumferential vascularization), whereas the tibiotarsi and tarsometatarsi had larger amounts of reticular organized bone tissue suggestive of more rapid osteogenesis (de Margerie *et al.*, 2004). The fibulae studied had the most extensive development of Haversian bone tissue (for more details, see the section below on the histological variation in the fibula).

The variable microanatomy and histology of the different bones suggests that bone deposition is influenced by localized growth rates (Chinsamy-Turan, 2005), modelling changes (Enlow, 1962) and/or the different biomechanical stresses experienced by the skeletal elements (Martin & Burr, 1989). The changes observed in the cross-sections in different parts of the compacta highlight the limitations of studying the histology of cores for deducing life-history data of extinct taxa.

Our study also provides pertinent insight into the histovariability and growth dynamics evident in the femora, tibiotarsi, tarsometatarsi and fibulae of aepyornithids. Below, we discuss: (1) the histology and growth dynamics evident in each of the hindlimb skeletal elements across the taxa studied; (2) the growth dynamics of aepyornithids in comparison to other ornithurine birds; (3) calcium mobilization in aepyornithids (which includes a discussion concerning reproductive demands of calcium in these giant birds); and (4) inclusions within a tarsometatarsus of a juvenile aepyornithid.

HISTOLOGICAL VARIABILITY IN AEPYORNITHID FEMORA

In the only detailed study of an embryo of *Aepyornis*, Balanoff & Rowe (2007) determined that the individual had almost completed the embryonic stage. Detailed morphological descriptions and measurements were made of the embryonic skeleton.

development of intracortical remodelling. E, higher magnification of the boxed region in panel D, showing overlapping generations of secondary osteons.

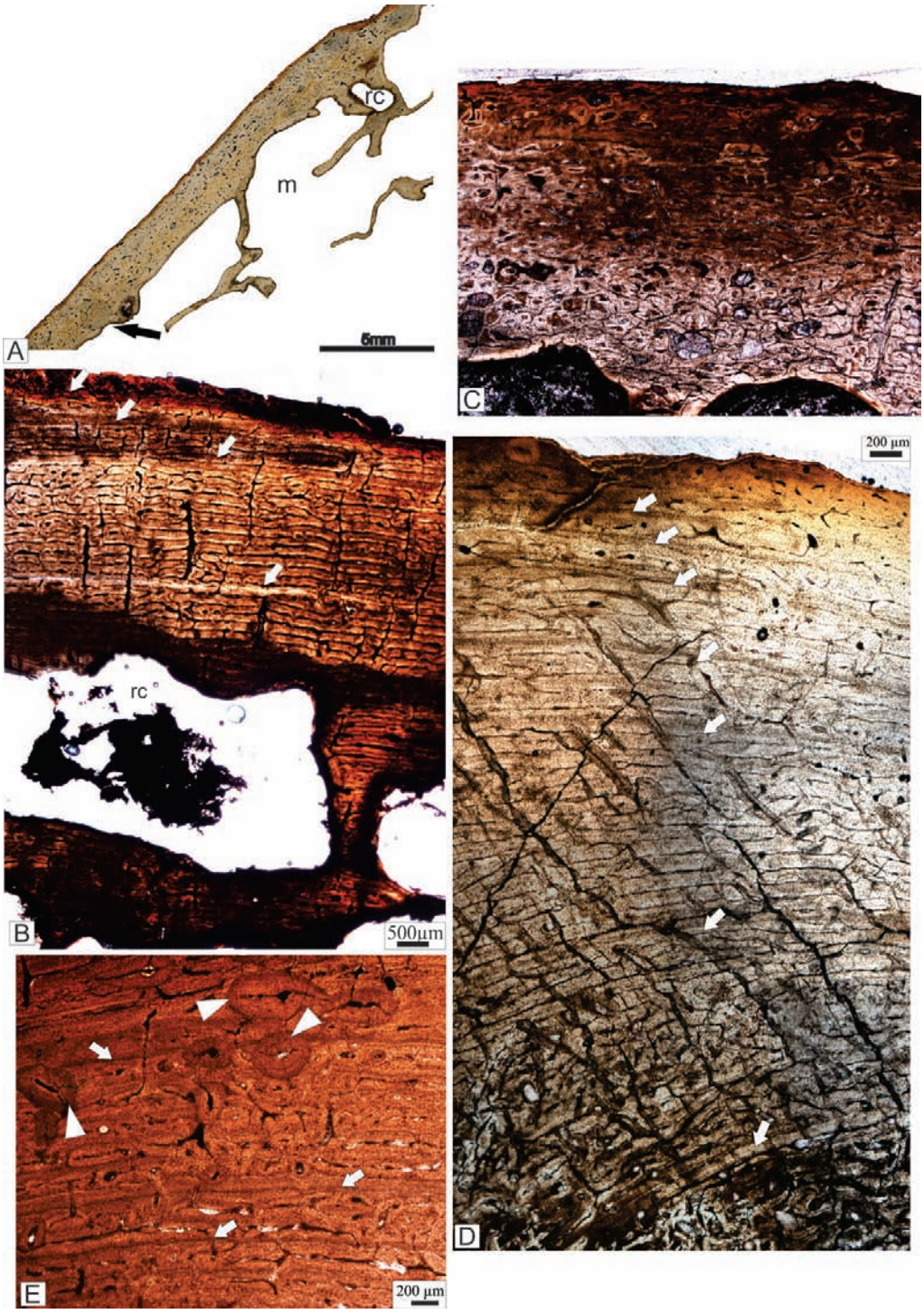

Figure 10. Femur NHMW 2014/0238/0046, transverse section. A, a low-magnification image, showing the compacta, with extensive bone remodelling in the perimedullary regions. Note the large resorption cavity (rc), the uneven, resorptive endosteal bone margin (arrow) and the narrow trabeculae that extend into the medullary cavity (m). B, higher magnification, showing the laminar fibrolamellar bone tissue interrupted by at least four growth rings (arrows). Abbreviation: rc, resorption cavities. C, femur NHMW 2014/0238/0047, showing the bone wall, with many secondary osteons located near the perimedullary region. Note the resorptive margin of the endosteal region. D, E, tibiotarsus NHMW 2014/0238/0017, transverse section. D, overall view of the compact bone wall, showing several growth rings (arrows) that interrupt the predominantly primary fibrolamellar bone tissue. E, higher magnification of the outer part of the bone wall, showing narrow annuli (arrows) that interrupt the fibrolamellar bone tissue and several secondary osteons (arrowheads) that occur throughout the cortex.

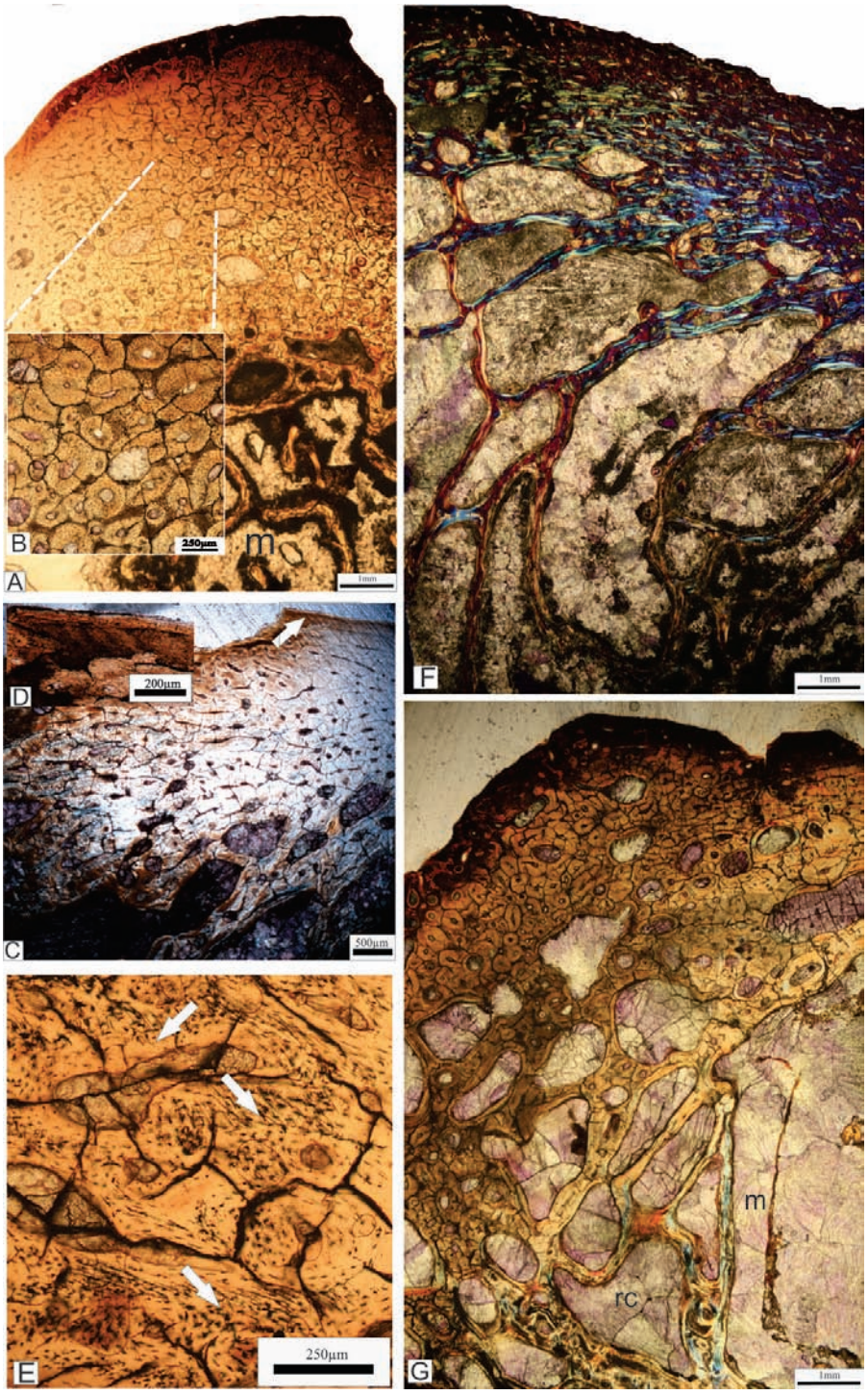

Figure 11. Fibula, NHMW 2014/0238/0051, transverse section. A, lateral part of the bone wall, showing extensive intracortical remodelling throughout the cortex. Notice the increasingly larger resorption cavities that develop towards the medullary cavity (m) and the increasingly cancellous texture of the bone wall towards the medullary cavity. B, higher magnification of the region indicated in panel A, showing dense Haversian bone. C, a section of the anterior-medial part of the bone wall, showing a narrow region of lamellar bone (arrow) in the outermost part of the compacta. Below this region is heavily reconstructed bone tissue, with many secondary osteons, in addition to enlarged cavities, with some containing narrow deposits of lamellar bone. D, higher magnification of the boxed region in panel C, showing the narrow band of lamellar bone tissue. E, nearer the medullary cavity is a region of secondary remodelled bone tissue with patches of Sharpey's fibres (arrows).

Most of the elements were unfused, and among the limb bone elements, the epiphyses of the bones were also not preserved (because at this stage of development they would largely have been made up of cartilage, which would have decayed rapidly after death; Chinsamy-Turan, 2005). The maximal width of the femur of this late-stage embryo is 1.5 cm, whereas the width of the smallest femur in our sample (NHMW 2014/0235/0052; Table 1) measures 4.5 cm. Considering that Brand *et al.* (2017) have found that the leg length of ostrich embryos increase by nearly 30% between 80 and 90% of incubation, it is possible that NHMW 2014/0235/0052 is a young hatchling. Indeed, this femur shows a distinct change in the type of bone tissue in the cortex, i.e. it has an inner band of reticular FLB that is separated by an LAG from an outer band consisting of laminar FLB. We propose that this LAG is a hatching line (Castanet & Smirina, 1990) and that the reticular FLB seen in the deep cortex was formed during embryonic growth and started to be resorbed by the expansion of the medullary cavity and the growth in diameter of the femoral shaft. Studies on modern birds have shown that among fibrolamellar bone tissues, reticular bone tissue is deposited at faster rates than fibrolamellar bone tissue with circumferential and/or longitudinal canals (e.g. Castanet *et al.*, 2000; de Margerie *et al.*, 2004). Unfortunately, we cannot analyse whether the perimeter enclosed by this hatching line coincides with the circumference of a femur of a newly hatched indvidual (Gonzáles *et al.*, 2019), because no hatchling aepyornithid specimens are known.

The resorptive inner margin of the bone clearly demonstrates that the bone formed during the earliest stages of life was actively resorbed owing to the expansion of the medullary cavity associated with the growth in diameter of the femur. The bone tissue appears to have been deposited rapidly at the periosteal margin. The large open canals visible are typical of the way in which fibrolamellar bone forms in young, fast-growing individuals [e.g. as seen in the embryonic Mesozoic bird, *Gobipteryx* (Chinsamy, 2002), hatchling Japanese quail (Starck & Chinsamy, 2002) or the king penguin, *Aptenodytes patagonicus* (de Margerie *et al.*, 2004)]. Here, a scaffold of woven bone matrix is laid down rapidly and encloses large spaces, in which vascular canals and other soft tissues are located (Starck & Chinsamy, 2002). Later, these spaces are filled by the slow deposition of endosteal lamellar bone tissue to form primary osteons (Francillon-Vieillot *et al.*, 1990; Chinsamy-Turan, 2005).

Our finding of the earlier-formed reticular fibrolamellar bone tissue nearest the medullary cavity in the smallest and probably youngest aepyornithid specimen in our sample, femur NHMW 2014/0238/0052, suggests that the earliest stages of all the aepyornithids was probably characterized by such rapid rates of osteogenesis.

Femoral histology of adult Aepyornithidae

In general, the present study found that the femora principally consisted of primary bone tissue in the outer part of the cortex, although bone resorption (eventually followed by subsequent redeposition of endosteal lamellar bone tissue later in ontogeny) was extensive in the perimedullary region. In all the femora, perimedullary resorption had led to the formation of enlarged cavities and to the development of bony struts with cores made of primary FLB bone tissue. Some secondary osteons formed during late ontogenetic stages in the cortex. However, these were relatively small and scattered and were mainly located in the perimedullary region. Nevertheless, we found differences between the *A. maximus* and *V. titan* femora, in that although they were similar in size, the latter showed more extensive secondary reconstruction, whereas the former tended to have predominantly primary periosteal bone. This could be indicative of taxonomic differences between these two aepyornithids or it could be a result of different ages (older adults are likely to show more Haversian tissue than younger ones).

Interestingly, in an earlier study of two large femora ascribed to *Aepyornis* [de Ricqlès *et al.*, 2016: MAD 378 (MNHN 1908-5 from an unknown locality) and MAD 364 (MNHN 1931–6 from Ankazoabo locality), with diameters of 8 and 8–9 cm, respectively], it was reported that MAD 378 showed no Haversian reconstruction, whereas the slightly larger MAD 364 was 'entirely reworked'. Based on the results obtained in our study of *A. maximus* and *V. titan* femora, we propose that the extensive development of Haversian bone in the femur MAD 364 suggests that it is most likely to be that of *V. titan*.

The present study shows that in both the unidentifiable aepyornithid femoral specimens and in the *A. hildebrandti* femur (NHMW 2014/0238/0038), growth marks (annuli) periodically interrupted the

G, anteromedial section of the bone wall, with a narrow region of compact bone wall that is heavily reconstructed. Many of the enlarged cavities reach cancellous proportions in the perimedullary region. F, fibula NHMW 2014/0238/0050, transverse section, showing the extensively remodelled bone tissue. The compact bone wall consists essentially of secondary bone. Several large resorption cavities (rc) are visible, and these become increasingly larger nearer the medullary cavity (m).

deposition of a predominantly primary laminar fibrolamellar bone tissue. In the three largest aepyornithid femora (FM2 and FM3 of *A. maximus* and FM1 of *V. titan*) we found that although they were estimated to be from individuals of similar body size, the *Vorombe* femur showed fewer growth marks in the femoral cortex and growth marks occurred more frequently in FM2 (*A. maximus*).

In *Vorombe* FM1 (one of the largest aepyornithid femora studied), where the external periosteal surface is preserved, it is uneven, suggesting that the bone is still growing in diameter at this stage of ontogeny (Enlow, 1962). Reticular FLB is also evident at the peripheral margin of the bone (Fig. 8B), suggesting that osteogenesis had not yet slowed down in this individual. In contrast, the largest femur in our sample (in terms of length and width of the proximal end) is *A. maximus* FM2, which shows fewer vascular canals and a distinctive textural shift in the bone tissue near the periphery, suggesting that the rate of bone deposition had drastically slowed down and that terminal growth had been attained (Fig. 6A, B). These histological features are in agreement with the macroscopic observation of well-ossified articular ends of the bone and indicate that this element is from an individual that had attained its adult body size. The two *A. maximus* femora vary in terms of the number of growth marks (i.e. annuli and/or LAGs) present in the cortex, and only femur FM2 shows an unusual woven tissue within the cancellous spaces around the medullary cavity (Fig. 6E, F; see later section on calcium metabolism). Also, FM2 shows the reconstructed trabecular bone, whereas although FM3 shows large eroded spaces, the resulting trabeculae are not reconstructed.

Histological variability in the Aepyornithidae tibiotarsi

Using the equations of Campbell & Marcus (1992), we estimated that the individual associated with the smallest tibiotarsus (NHMW 2014/0238/0015, with clearly unfinished articular ends) in our sample had a body mass of 86 kg (Tables 1). The histology of this bone was variable in different parts of the diaphyseal cross-section, with the posterior region of the bone wall having two annuli that interrupted the deposition of fibrolamellar bone tissue. However, it is possible that earlier growth rings might have been obliterated owing to medullary expansion or simply remodelling in the perimedullary region. The localized abundance of secondary osteons in the lateral region suggests that this region corresponds to an area of muscle insertion, and it is likely that the variable histology reflects different loading regimens (e.g. McFarlin *et al.*, 2008), i.e. an adaptive response to fatigue microdamage caused by loading strain in this region (e.g. Martin & Burr, 1989), while the cement lines around the secondary osteons serve to resist the propagation of microcracks (Martin & Burr, 1989; Mohsin, *et al.*, 2006). It is also worth noting that Enlow (1962) had found that intracortical remodelling was also often correlated with soft tissue attachment areas. The variability of the bone tissue across the cross-section highlights the limitations of using only cores to describe the bone tissue of individuals. The large amount of compacted coarse cancellous bone in the cross-section is attributable to the relocation of the metaphyseal regions of earlier growth stages into the diaphysis of older individuals (Enlow, 1962) and cautions against using sections that are closer to the metaphysis as opposed to the midshaft region.

Specimen NHMW 2014/0238/0009 (also with unfinished articular ends) is from a slightly larger juvenile individual, and we estimated its body mass as ~97 kg (Table 1). Its bone histology indicates that it is still undergoing rapid appositional growth, and the large amount of compact coarse cancellous bone tissue present (Figure 4) indicates that the metaphysis of an earlier stage had been relocated into the shaft of the tibiotarsus (Enlow, 1962), which suggests that the bone was also rapidly increasing in length. Intracortical remodelling is further developed at this stage of growth, but does not extending to the outer cortex. Three growth rings (annuli) are present, but here too, earlier growth rings might have been removed owing to medullary expansion and modelling of the bone.

As seen in the Aepyornithidae femora, the tibiotarsi all show histological variability across the cross-section, but consistently among all the different taxa there appears to be a high amount of secondary reconstruction and, in many cases, erosion cavities and secondary osteons interrupt the growth marks. However, secondary reconstruction is never intensive enough to obliterate all traces of the growth marks completely. Towards the perimedullary regions there appear to be a larger number of enlarged erosion cavities. There appears to be some variation in the extent of secondary reconstruction in the bone walls of the different specimens. This might be linked to phosphocalcic metabolism and to responses to the stresses and strains experienced (e.g. Martin & Burr, 1989) and/or be indicative of sites of muscle attachment (Enlow, 1962).

Histological variation in the Aepyornithidae tarsometatarsi

The smallest individual in our sample (NHMW 2014/0238/0049) showed variable histology across the thin section, suggesting that from early in ontogeny different parts of the cross-section experienced

different growth rates and loading forces. The overall extensive intracortical remodelling that resulted in the development of secondary osteons distributed throughout the cortex right up to the peripheral margin suggests that the tarsometatarsus experiences a completely different loading regimen in comparison to the femur and the tibiotarsus. This contrasts with the recent findings that different limb bones in equids presented comparable degrees of bone remodelling, although those researchers found that environmental differences (which probably imposed different stresses) influenced the extent of intracortical remodelling in the metapodial elements (Martinez-Maza *et al.*, 2014).

The tarsometatarsus NHMW 2014/0238/0048 (and those from the taxonomically unidentifiable juvenile samples) has unfinished proximal and distal articular surfaces and, like the tarsometatarsi of *A. hildebrandti* (NHMW 2014/0238/0034 and NHMW 2014/0238/0036) and *A. maximus* (NHMW 2014/0238/0033), preserves a similar bone tissue to that described in the previous subsection. In specimen NHMW 2014/0238/0034, parts of the compacta are densely packed with secondary osteons and localized areas have dense Haversian bone. In this specimen, there are very limited occurrences of primary bone in the compacta. A large tarsometatarsus we sampled was that of *Vorombe* (MNHN TMT1), which showed a slightly reduced vascularization in the peripheral region, suggesting a slowing down in the rate of bone deposition, and a clear reduction in the extent of secondary reconstruction, which might be indicative of being close to skeletal maturity. The largest specimen (*V. titan* TMT2) shows extensive secondary reconstruction and the development of dense Haversian bone. The tarsometatarsus studied by de Ricqlès *et al.* (2016) was probably from an even larger individual, because it was described as having dense Haversian bones, with many trabeculae in the medullary cavity.

It is apparent that the tarsometatarsus undergoes more reconstruction as compared to the femora. Indeed, in most terrestrial birds, the tarsometatarsus is recognized as the skeletal element in the limb that experiences the greatest stresses and strains during locomotion (Storer, 1960; Angst *et al.*, 2016), and the highly remodelled cortex of these bones in Aepyornithidae suggests that they experienced high biomechanical loading.

Histological variation in the fibula

The fibula appears to be the element that experienced the most significant amount of secondary reconstruction. Dense Haversian bone is common in the cortex (Fig. 8), suggesting that this bone, together with the tibia, bore substantial mechanical strain. It is also possible that the extensive remodelling reflects its smaller relative size in comparison to the other limb elements (Padian *et al.*, 2016).

Growth dynamics of Aepyornithidae compared with other ornithurine birds

Aepyornithidae are represented by taxa that have body sizes ranging from medium to large, with *V. titan* having the distinction of being one of the largest birds that ever lived (Murray & Vickers-Rich, 2004; Hansford & Turvey, 2018), rivalled only by the Australian mihirung, *Dromornis*, in terms of its grand stature and body mass. All aepyornithid bones studied suggest that they grew in periodic spurts throughout ontogeny. This contrasts with the predominant ornithurine growth dynamics of rapid uninterrupted growth to adult body size (in < 1 year, hence the absence of growth marks; (Enlow, 1963; Chinsamy *et al.*, 1994; Starck & Chinsamy, 2002). However, it has been recognized that in certain circumstances, such as on islands or in long-lived taxa, growth of ornithurine birds can be interrupted periodically during ontogeny (Starck & Chinsamy, 2002). This has been documented, for example, in several ratites from New Zealand, such as the giant moa *Dinornis* (Turvey *et al.*, 2005) and the kiwi *Apteryx* (Bourdon *et al.*, 2009), the extinct Mesozoic bird *Gargantuavis* (Chinsamy *et al.*, 2014), the Cenozoic *Gastornis* (synonym to *Diatryma*; de Ricqlès *et al.*, 2001), the dodo (Angst *et al.*, 2017) and, albeit not insular, the long-lived parrot *Amazona amazonica* (de Ricqlès *et al.*, 2001). Thus, as proposed by Starck & Chinsamy (2002), although the plesiomorphic growth pattern for tetrapods might have been flexible developmental trajectories, the reduction in body size and shortening of the growth period in ornithurine birds to < 1 year (Starck & Ricklefs, 1998; Starck & Chinsamy, 2002) might have led to the rapid uninterrupted growth dynamics that usually characterize ornithurines. However, in the absence of predators and/or limitations of food resources, and when the selection for rapid growth is reduced (such as on islands), birds (e.g. giant moa, Turvey *et al.*, 2005; the kiwi, Bourdon *et al.*, 2009; *Gargantuavis*, Chinsamy *et al.*, 2014; the dodo, Angst *et al.*, 2017) and mammals (e.g. *Myotragus*, Köhler & Moyà-Solà, 2009) can resort to flexible plesiomorphic growth dynamics (Chinsamy-Turan, 2005).

Why did aepyornithids form growth rings in their bones?

In a study of wild ruminants from tropical to polar environments, Köhler *et al.* (2012) showed that growth was cyclical and dependent on seasonal environmental conditions, i.e. during the unfavourable season the growth of the animals was arrested and they experienced a decrease in body temperature, metabolic rate and bone-growth factors. However, during the favourable season, they experienced higher growth

and metabolic rates, indicating efficiency in using seasonal resources.

Most of the aepyornithid material we studied was recovered from Antsirabe, a locality in the central highlands, ~100 km North of Antananarivo. Climate data for Antananarivo show strong seasonality, with wet winters and minimal temperatures < 10 °C. Given that Antsirabe is at a slightly higher elevation, it would have been cooler and possibly wetter. Interestingly, there are several mammalian taxa from Madagascar that show seasonal growth patterns; for example, tenrecs and mouse lemurs are known to experience torpor, and ring-tailed lemurs also show seasonal growth patterns (Overdorff, 1993; Pereira, 1993; Ganzhorn, 2002; Randrianambinina *et al.*, 2003). It is therefore likely that the growth rings evident in the compacta of the bones of the aepyornithid indicate that they experienced seasonal growth rates in response to the seasonal environmental conditions. Furthermore, isotope analyses by Clarke *et al.* (2006) suggested that aepyornithids were browsers of C_3 plants, which probably lost their leaves in winter, thus resulting in decreased food availability that might also have contributed to the periodic decrease in overall growth evident in these birds.

Mobilization of calcium from bones

The localized concentration of secondary osteons in the compacta of many of the bones suggests that they are linked to the biomechanical demands of the skeletal element (e.g. McFarlin *et al.*, 2008), whereas more generalized intracortical remodelling (erosion cavities, cavities with secondary deposits of bone and secondary osteons) that develops throughout the cortex might be more related to general calcium metabolism, age and moulting (e.g. Meister, 1951; Dabee, 2014; Angst *et al.*, 2017).

de Ricqlès *et al.* (2016) originally proposed that there appears to be a proximodistal gradient in terms of secondary reconstruction, with the more distal elements showing more extensive remodelling. In our study, although the femora generally consisted of primary periosteal bone, the fibula showed the most extensively developed intracortical remodelling of all the limb elements studied. It is possible that the development of secondary reconstruction in these elements is linked to the fact that the fibulae are much smaller, non-weightbearing bones in rapidly growing individuals (Padian *et al.*, 2016).

Calcium demands during reproduction

Given the large size of aepyornithid eggs, calcification thereof would have imposed high demands for calcium in reproductive females. Interestingly, among birds, calcium is usually mobilized from medullary bone formed during ovulation within the medullary cavity of skeletal elements (e.g. Chinsamy-Turan, 2005; Schweitzer *et al.*, 2005; Chinsamy *et al.*, 2013; Canoville *et al.*, 2019). However, in our study of aepyornithids and in the earlier study by de Ricqlès *et al.* (2016), none of the bones studied showed the endosteally formed spiculate, cancellous-textured, woven bone often described as medullary bone (e.g. Dacke *et al.*, 1993; Chinsamy-Turan, 2005; Schweitzer *et al.*, 2005). This is not surprising, because medullary bone formation is under the direct influence of oestrogen (Miller & Bowman, 1981), and it is formed naturally only in an ovulating female bird or at a stage in the reproductive cycle of the female bird when egg shelling has not been completed. Thus, owing to its ephemeral nature, the probability of finding such bone tissue among fossil birds is low.

Interestingly, in the study of two tibiotarsi of *Aepyornis*, de Ricqlès *et al.* (2016) reported a large amount of compact endosteal deposits of lamellar tissue showing several cycles of resorption and re-deposition, which produced incomplete 'endosteal osteons'. These endosteal deposits were hypothesized by de Ricqlès *et al.* (2016) to be related to the high demands for calcium during reproduction. Indeed, in our aepyornithid samples studied, we also found several such repeated deposits of lamellar bone along the endosteal parts of the compacta and on the trabeculae of various limb bones. However, in contrast to de Ricqlès *et al.* (2016), we suggest that this episodically formed endosteal tissue is not formed in response to reproductive demands of calcium, because such bone tissues have been observed in in the humeri, radii, femora and tibiae of adult male and female giraffes (*Giraffa camelopardalis*) (Caitlin Smith, personal communication, University of Cape Town, MSc. research, 2020). Although a few long bones of subadult giraffes showed this tissue, it was not apparent in any of the bones of young juveniles, which leads us to suggest that this tissue might possibly be related to the attainment of large body size.

Curiously, in one of the *A. maximus* femora studied (FM2) an unusual infilling of woven bone tissue within cancellous spaces in the subendosteal region of the cortex was observed. This finely textured woven bone tissue has a rich supply of simple blood vessels and, in some places, it appears that this bone was actively resorbed. Could this unusual endosteal tissue be homologous to avian medullary bone? Usually, medullary bone forms as a trabecular and woven bone tissue that extends from the endosteal margin of the inner circumferential layer into the medullary cavity (e.g. Dacke *et al.*, 1993; Chinsamy-Turan, 2005; Schweitzer *et al.*, 2005). However, Whitehead (2004) has reported that often during the egg-laying period,

female hens resorb structural bone and, instead of forming secondary osteons, the osteoblasts can deposit woven textured medullary bone as spicules from the endosteal surface. Canoville *et al.* (2019) also documented that medullary bone can be deposited within resorption cavities in the perimedullary region of birds. It is possible that this might be what we are seeing in *Aepyornis*, i.e. the secondarily formed tissue infilling vacant resorption cavities, which were formed as a result of the demand for calcium during eggshelling. Chinsamy *et al.* (2016) described unusual, possibly pathological, deposits of vascularized endosteal bone in three bones of saltasaurine dinosaurs, but it should be noted that the endosteally formed tissue in *A. maximus* FM2 (MNHN) is woven bone as opposed to the vascularized lamellar bone described in some the armoured dinosaurs. The enigmatic tissue in *Aepyornis* also differs from the pathological endosteal deposits observed in *Mussaurus* (Cerda *et al.*, 2014), which, although woven tissue, contains high concentrations of osteocyte lacunae that are typical of pathologies.

Thus, we propose that it is likely that the secondarily formed tissue within the vacant cavities in the perimedullary regions in *A. maximus* is indeed a type of medullary bone (or at least related to the high calcium homeostasis during egg laying), even though it does not have the spicular or honeycomb-like microstructure often ascribed to medullary bone in the published literature (e.g. Whitehead, 2004; Chinsamy-Turan, 2005; Schweitzer *et al.*, 2005; Canoville *et al.*, 2019). Given that no medullary bone is observed within the medullary cavity, it also suggests that this individual had already laid eggs or was at a late stage in the egg-shelling process.

Inclusions within a juvenile aepyornithid tarsometatarsus

The fortuitous finding of the root tissue and fragments of other plant matter within the medullary cavity of a juvenile tarsometatarsus (NHMW 2014/0238/0049) is curious. Although it is not commonly reported, it is possible that externally derived material, such as plant matter and other inclusions (Chinsamy-Turan, 2005), can enter the medullary cavity and pore spaces in bones through post-mortem cracks in the bone wall during burial and/or fossilization. Such inclusions are sometimes useful in gleaning information about the biology, ecology and taphonomy of the fossilized animal. Chinsamy *et al.* (1997) has previously reported on *Podocarpus* wood fragments within the medullary cavity of a Cretaceous-aged polar dinosaur femur from Dinosaur Cove in Australia. Fungal traces have also been identified in Permian-aged therocephalian bones from the Karoo basin of South Africa (Chinsamy-Turan & Ray, 2012).

Concluding remarks

This comprehensive assessment of the osteohistology of aepyornithids, in conjunction with a previous study by de Ricqlès *et al.* (2016), has highlighted significant histological variability among hindlimb elements. Our results show that generally, although the femur undergoes the least amount of secondary reconstruction, it does not retain a good record of growth during early ontogeny because of substantial perimedullary resorption/remodelling (Enlow, 1963). However, our results show that although all the skeletal elements studied undergo some degree of secondary reconstruction and remodelling, the tibiotarsus provides the best record of growth throughout ontogeny.

Our histological observations of an endosteal woven bone tissue within the cancellous spaces around the medullary cavity in an *A. maximus* femur suggest that this might be remnants of a tissue homologous to avian medullary bone, which serves as a reservoir of calcium to form the eggshell (e.g. Dacke *et al.*, 1993). Furthermore, the finding of reconstructed endosteal lamellar bone around the medullary cavity and along trabeculae in male and female specimens of modern giraffes refutes the previous hypothesis that these histological features in aepyornithids are the result of reproductive demands of calcium on females during egg laying (de Ricqlès *et al.*, 2016).

The histology of aepyornithid bones (irrespective of the different body sizes) shows that they experienced alternating periods of rapid and slow rates of growth. The most rapid phase of growth appears to be during the early stages of ontogeny, i.e. during the embryonic stages, when reticular fibrolamellar bone tissue is predominantly deposited. For older aepyornithids, the rate of osteogenesis is slightly reduced but nonetheless high enough to form laminar fibrolamellar bone tissue. As reported by de Ricqlès *et al.* (2016), we also found that *A. maximus* femora exhibited large radial canals that traverse the cortex and interlink the vascular canals in the laminae. Such features have been observed in the cortices of long bones of modern giraffe specimens (Caitlin Smith, personal communication 2020) and they might be related to large body size and the need for rapid assimilation of nutrients and the removal of waste products. The rapid rates of growth are interrupted periodically by annuli or LAGs. In the latest stages of ontogeny (as suggested by *A. maximus*, FM2), the rate of growth decreases substantially to result in the deposition of periodically interrupted lamellar bone tissue. Our osteohistology results from *A. maximus*, *A. hildebrandti* and *V. titan*, in addition to unidentifiable elephant bird taxa, show that

Aepyornithidae, like other insular birds, experienced protracted developmental trajectories, i.e. taking several years to reach skeletal maturity. We suggest that seasonality combined with food availability might have resulted in the periodic interruptions of growth evident in their bones.

ACKNOWLEDGEMENTS

James Hansford is thanked for kindly assisting us with the taxonomic identification of our study specimens of Aepyornithidae. Anton Fürst (NHMW) is thanked for sampling the specimens at NHMW. We are grateful to Ronan Allain (curator for the dinosaurs and fossil birds in the MNHN Paris) for the access to the specimens, and Eric Buffetaut is thanked for help with the core sampling of these specimens. Caitlin Smith, University of Cape Town is acknowledged for sharing information from her yet unpublished MSc. research. Sibongile Fatyi is acknowledged for assisting A. Ch. with the thin section preparation at the University of Cape Town (UCT). We acknowledge Jurgen Geitner from the UCT Pathology Learning Centre for the use of the Olympus VS120 virtual microscope, and palaeobotanist Ari Iglasias for confirming our identification of the plant matter in the medullary cavity of the juvenile tarsometarsus. The work was funded by the National Research Foundation (NRF), South Africa, Africa Origins Platform, grant number 117716 to A. Ch.

A.Ch. wrote the first draft of the manuscript, took all the photomicrographs and compiled the plates; D.A. and A.C. measured and sampled specimens in MNHN Paris. U.G. measured and sampled specimens at NHMW; D.A. compiled the bibliography for the manuscript, and D.A., U.G. and A.C. commented on an earlier draft of the manuscript.

REFERENCES

Amadon D. 1947. An estimated weight of the largest known bird. *The Condor* **49:** 159–164.

Andrews CW. 1894a. Note on a new species of *Æpyornis* (*Æ Titan*). *Geological Magazine* **1:** 18–20.

Andrews CW. 1894b. On some remains of *Aepyornis* in the British Museum (Nat. Hist.). *Proceedings of the Royal Society of London* **1894:** 108–123.

Andrews CW. 1896. On the skull, sternum, and shoulder-girdle of *Aepyornis*. *Ibis* **2:** 376–389.

Andrews CW. 1897. Note on a nearly complete skeleton of *Aepyornis* from Madagascar. *Geological Magazine* **4:** 241–250.

Angst D, **Buffetaut E. 2017.** *Paleobiology of giant flightless birds*. London, Oxford: ISTE Press Elsevier.

Angst D, **Buffetaut E**, **Lécuyer C**, **Amiot R. 2016.** A new method for estimating locomotion type in large ground birds. *Palaeontology* **59:** 217–223.

Angst D, **Buffetaut E**, **Lécuyer C**, **Amiot R**, **Smektala F**, **Giner S**, **Méchin A**, **Méchin P**, **Amoros A**, **Leroy L. 2014.** Fossil avian eggs from the Palaeogene of southern France: new size estimates and a possible taxonomic identification of the egg-layer. *Geological Magazine* **152:** 70–79.

Angst D, **Chinsamy A**, **Steel L**, **Hume JP. 2017.** Bone histology sheds new light on the ecology of the dodo (*Raphus cucullatus*, Aves, Columbiformes). *Scientific Reports* **7:** 7993.

Balanoff AM, **Rowe T. 2007.** Osteological description of an embryonic skeleton of the extinct elephant bird, *Aepyornis* (Palaeognathae: Ratitae). *Journal of Vertebrate Paleontology* **27:** 1–53.

Berger R, **Ducote K**, **Robinson K**, **Walter H. 1975.** Radiocarbon date for the largest extinct bird. *Nature* **258:** 709.

Bond WJ, **Silander JA. 2007.** Springs and wire plants: anachronistic defences against Madagascar's extinct elephant birds. *Proceedings of the Royal Society B: Biological Sciences* **274:** 1985–1992.

Bourdon E, **Castanet J**, **de Ricqlès A**, **Scofield P**, **Tennyson A**, **Lamrous H**, **Cubo J. 2009.** Bone growth marks reveal protracted growth in New Zealand kiwi (Aves, Apterygidae). *Biology Letters* **5:** 639–642.

Brand Z, **Cloete SW**, **Malecki IA**, **Brown CR. 2017.** Ostrich (*Struthio camelus*) embryonic development from 7 to 42 days of incubation. *British Poultry Science* **58:** 139–143.

Burckhardt R. 1893. Über *Aepyornis*. Paeontologische Abhandlungen **2:** 127–145.

Burney D, **James H**, **Grady F**, **Rafamantanantsoa JG**, **Wright H**, **Cowart J. 1997.** Environmental change, extinction and human activity: evidence from caves in NW Madagascar. *Journal of Biogeography* **24:** 755–767.

Burney DA. 1997. Theories and facts regarding Holocene environmental change before and after human colonization. In: Goodman SM, Patterson BD, eds. *Natural change and human impact in Madagascar*. Washington: Smithsonian Institution Press, 75–89.

Burney DA, **Burney LP**, **Godfrey LR**, **Jungers WL**, **Goodman SM**, **Wright HT**, **Jull AT. 2004.** A chronology for late prehistoric Madagascar. *Journal of Human Evolution* **47:** 25–63.

Campbell KE Jr, **Marcus L. 1992.** The relationship of hindlimb bone dimensions to body weight in birds. *Natural History Museum of Los Angeles County Science Series* **36:** 395–412.

Canoville A, **Schweitzer MH**, **Zanno LE. 2019.** Systemic distribution of medullary bone in the avian skeleton: ground truthing criteria for the identification of reproductive tissues in extinct Avemetatarsalia. *BMC Evolutionary Biology* **19:** 71.

Castanet J, **Rogers KC**, **Cubo J**, **Boisard JJ. 2000.** Periosteal bone growth rates in extant ratites (ostriche and emu). Implications for assessing growth in dinosaurs. *Comptes rendus de l'Academie des sciences. Serie III, Sciences de la vie* **323:** 543–550.

Castanet J, **Smirina E. 1990.** Introduction to the skeletochronological method in amphibians and reptiles. *Annales des Sciences Naturelles* **11:** 191–196.

Cerda IA, **Chinsamy A**, **Pol D. 2014.** Unusual endosteally formed bone tissue in a Patagonian basal sauropodomorph dinosaur. *Anatomical Record* **297:** 1385–1391.

Chinsamy A. 1995. Histological perspectives on growth in the birds *Struthio camelus* and *Sagittarius serpentarius*. *Courier Forschungsinstitut Senckenberg* **181:** 317–323.

Chinsamy A. 2002. Bone microstructure of early birds. In: Chiappe LM, Witmer LM, eds. *Mesozoic birds: above the heads of dinosaurs*. Berkeley, Los Angeles, London: University of California Press, 421–431.

Chinsamy A, **Buffetaut E**, **Canoville A**, **Angst D. 2014.** Insight into the growth dynamics and systematic affinities of the Late Cretaceous *Gargantuavis* from bone microstructure. *Die Naturwissenschaften* **101:** 447–452.

Chinsamy A, **Cerda I**, **Powell J. 2016.** Vascularised endosteal bone tissue in armoured sauropod dinosaurs. *Scientific Reports* **6:** 24858.

Chinsamy A, **Chiappe L**, **Dodson P. 1994.** Growth rings in Mesozoic avian bones: physiological implications for basal birds. *Nature* **368:** 196–197.

Chinsamy A, **Chiappe LM**, **Marugán-Lobón J**, **Chunling G**, **Fengjiao Z. 2013.** Gender identification of the Mesozoic bird *Confuciusornis sanctus*. *Nature Communications* **4:** 1381.

Chinsamy A, **February E**, **Harley E**, **Rich T**, **Vickers-Rich P. 1997.** Wood within a polar dinosaur bone. *South African Journal of Science* **93:** 48.

Chinsamy A, **Raath MA. 1992.** Preparation of fossil bone for histological examination. *Paleontology of Africa* **29:** 39–44.

Chinsamy-Turan A. 2005. *The microstructure of dinosaur bone: deciphering biology with fine-scale techniques.* Baltimore: John Wiley & Sons.

Chinsamy-Turan A. 2012. *The forerunners of mammals: radiation, histology, biology.* Bloomington: Indiana University Press.

Chinsamy-Turan A, **Ray S. 2012.** Bone histology of some therocephalians and gorgonopsians, and evidence of bone degradation by fungi. In: Chinsamy-Turan A, ed. *Forerunners of mammals.* Bloomington: Indiana University Press, 199–221.

Clarke SJ, **Miller GH**, **Fogel ML**, **Chivas AR**, **Murray-Wallace CV. 2006.** The amino acid and stable isotope biogeochemistry of elephant bird (*Aepyornis*) eggshells from southern Madagascar. *Quaternary Science Reviews* **25:** 2343–2356.

Cracraft J. 1974. Phylogeny and evolution of the ratite birds. *Ibis* **116:** 494–521.

Dabee VP. 2014. *Comparison of the long bone microstructure of two southern African marine birds, the Cape gannet (Morus capensis) and the African penguin (Spheniscus demersus) with respect to their aquatic adaptations.* Honours thesis, University of Cape Town.

Dacke CG, **Arkle S**, **Cook DJ**, **Wormstone IM**, **Jones S**, **Zaidi M**, **Bascal ZA. 1993.** Medullary bone and avian calcium regulation. *The Journal of Experimental Biology* **184:** 63–88.

Deeming DC. 1999. *Ostrich: biology, production and health.* Wallingford: CABI Publishing.

Enlow D. 1962. A study of the post-natal growth and remodeling of bone. *American Journal of Anatomy* **110:** 79–101.

Enlow DH. 1963. *Principles of bone remodeling: an account of post-natal growth and remodeling processes in long bones and the mandible*. Springfield, IL: Charles C. 'l'homas.

Enlow DH, **Brown SO. 1957.** A comparative histological study of fossil and recent bone tissues. Part II. *The Texas Journal of Science* **9:** 186–204.

Erickson GM. 2005. Assessing dinosaur growth patterns: a microscopic revolution. *Trends in Ecology & Evolution* **20:** 677–684.

Francillon-Vieillot H, **de Buffrénil V**, **Castanet J**, **Géraudie J**, **Meunier FJ**, **Sire JY**, **Zylberberg L**, **de Ricqlès A. 1990.** Microstructure and mineralization of vertebrate skeletal tissues. Chapter 20. In: Carter JG, ed. *Skeletal biomineralization: patterns, processes and evolutionary trends.* New York: Van Nostrand Reinhold, 471–548.

Fuller E. 1987. *Extinct birds.* New York: Facts on File.

Ganzhorn JU. 2002. Distribution of a folivorous lemur in relation to seasonally varying food resources: integrating quantitative and qualitative aspects of food characteristics. *Oecologia* **131:** 427–435.

Geoffrey Saint-Hilaire I. 1851. Des ossements et des oeufs trouvés à Madagascar, dans des alluvions modernes, et provenant d'un oiseau gigantesque. *Comptes Rendus Hebdomadaires des Séances de l'Académie des Sciences* **32:** 101–107.

Gommery D, **Sénégas F**, **Valentin F**, **Ramanivosoa B**, **Randriamantaina H**, **Kerloc'h P**, **Akiba M. 2011.** Madagascar: premiers habitants et biodiversité passé. *Archéologia* **494:** 40–49.

González R, **Cerda IA**, **Filippi LS**, **Salgado L. 2019.** Early growth dynamics of titanosaur sauropods inferred from bone histology. *Palaeogeography, Palaeoclimatology, Palaeoecology* **537:** 109404.

Goodman SM. 1999. Holocene bird subfossils from the sites of Ampasambazimba, Antsirabe and Ampoza, Madagascar: changes in the avifauna of south central Madagascar over the past few millennia. In: Adams NJ, Slotow RH, eds. *Proceedings of the 22nd International Ornithological Congress*. Johannesburg, South Africa: Bird Life, 3071–3083.

Goodman SM, **Jungers WL. 2013.** *Les animaux et écosystèmes de l'Holocene disparus de Madagascar.* Antananarivo: Association Vahatra.

Handley WD, **Chinsamy A**, **Yates AM**, **Worthy TH. 2016.** Sexual dimorphism in the late Miocene mihirung *Dromornis stirtoni* (Aves: Dromornithidae) from the Alcoota Local Fauna of central Australia. *Journal of Vertebrate Paleontology* **36:** e1180298.

Hansford JP, **Turvey ST. 2018.** Unexpected diversity within the extinct elephant birds (Aves: Aepyornithidae) and a new identity for the world's largest bird. *Royal Society Open Science* **5:** 181295.

Henrici P. 1957. Aepyornis-Eier. *Mitteilungen der Naturforschenden Gesellschaft in Bern* **14:** 135–139.

Köhler M, **Marín-Moratalla N**, **Jordana X**, **Aanes R. 2012.** Seasonal bone growth and physiology in endotherms shed light on dinosaur physiology. *Nature* **487:** 358–361.

Köhler M, **Moyà-Solà S. 2009.** Physiological and life history strategies of a fossil large mammal in a resource-limited environment. *Proceedings of the National Academy of Sciences of the United States of America* **106:** 20354–20358.

Lavauden L. 1931. Animaux disparus et légendaires de Madagascar. *Revue scientifique illustrée* **69:** 297–308.

Legendre LJ, **Bourdon E**, **Scofield RP**, **Tennyson AJ**, **Lamrous H**, **de Ricqlès A**, **Cubo J. 2014.** Bone histology, phylogeny, and palaeognathous birds (Aves: Palaeognathae). *Biological Journal of the Linnean Society* **112:** 688–700.

Mahé J, **Sourdat M. 1972.** Sur l'extinction des vertébrés subfossiles et l'aridification du climat dans le Sud-Ouest de Madagascar. *Bulletin de la Societe Geologique de France* **14:** 1–5.

de Margerie E, **Robin JP**, **Verrier D**, **Cubo J**, **Groscolas R**, **Castanet J. 2004.** Assessing a relationship between bone microstructure and growth rate: a fluorescent labelling study in the king penguin chick (*Aptenodytes patagonicus*). *The Journal of Experimental Biology* **207:** 869–879.

Martin RB, **Burr DB. 1989.** *Structure, function and adaptation of compact bone.* New York: Raven Press.

Martinez-Maza C, **Alberdi MT**, **Nieto-Diaz M**, **Luis Prado J. 2014.** Life-history traits of the Miocene Hipparion concudense (Spain) inferred from bone histological structure. *PLoS ONE* **9:** e103708.

McFarlin SC, **Terranova CJ**, **Zihlman AL**, **Enlow DH. 2008.** Regional variability in secondary remodeling within long bone cortices of catarrhine primates: the influence of bone growth history. *Journal of Anatomy* **213:** 308–324.

Meister W. 1951. Changes in histological structure of the long bones of birds during the molt. *The Anatomical Record* **111:** 1–21.

Miller SC, **Bowman BM. 1981.** Medullary bone osteogenesis following estrogen administration to mature male Japanese quail. *Developmental Biology* **87:** 52–63.

Milne-Edwards A, **Grandidier A. 1869.** Nouvelles observations sur les caractères zoologiques et les affinités naturelles de l'*Aepyornis* de Madagascar. *Annales des Sciences Naturelles* **7:** 85–114.

Mitchell KJ, **Llamas B**, **Soubrier J**, **Rawlence NJ**, **Worthy TH**, **Wood J**, **Lee MSY**, **Cooper A. 2014.** Ancient DNA reveals elephant birds and kiwi are sister taxa and clarifies ratite bird evolution. *Science* **344:** 898–900.

Mlíkovský J. 2003. Eggs of extinct aepyornithids (Aves: Aepyornithidae) of Madagascar: size and taxonomic identity. *Sylvia* **39:** 133–138.

Mohsin S, **O'Brien FJ**, **Lee TC. 2006.** Osteonal crack barriers in ovine compact bone. *Journal of Anatomy* **208:** 81–89.

Monnier L. 1913. Les *Aepyornis*. *Annales de Paléontologie* **8:** 125–167.

Murray PF, **Vickers-Rich P. 2004.** *Magnificent mihirungs. The colossal flightless birds of the Australian dreamtime*. Bloomington: Indiana University Press.

Overdorff DJ. 1993. Similarities, differences, and seasonal patterns in the diets of *Eulemur rubriventer* and *Eulemur fulvus rufus* in the Ranomafana National Park, Madagascar. *International Journal of Primatology* **14:** 721–753.

Padian K, **Werning S**, **Horner JR. 2016.** A hypothesis of differential secondary bone formation in dinosaurs. *Comptes Rendus Palevol* **15:** 40–48.

Pereira ME. 1993. Seasonal adjustment of growth rate and adult body weight in ringtailed lemurs. In: Kappeler PM, Ganzhorn JU, eds. *Lemur social systems and their ecological basis.* New York: Plenum press, 205–221.

Ponton F, **Elżanowski A**, **Castanet J**, **Chinsamy A**, **de Margerie E**, **de Ricqlès A**, **Cubo J. 2004.** Variation of the outer circumferential layer in the limb bones of birds. *Acta Ornithologica* **39:** 137–140.

Pycraft WP. 1900. On the morphology and phylogeny of the Palaeognathae (Ratitae and Crypturi) and Neognathae (Carinatae). *The Transactions of the Zoological Society of London* **15:** 149–290.

Rakotozafy LM, **Goodman SM. 2005.** *Contribution à l'étude zooarchéologique de la région du Sud-ouest et extrême Sud de Madagascar sur la base des collections de l'ICMAA de l'Université d'Antananarivo.* Taloha 14/15: Available at: http://www.taloha.info/document.php?id=181

Randrianambinina B, **Rakotondravony D**, **Radespiel U**, **Zimmermann E. 2003.** Seasonal changes in general activity, body mass and reproduction of two small nocturnal primates: a comparison of the golden brown mouse lemur (*Microcebus ravelobensis*) in Northwestern Madagascar and the brown mouse lemur (*Microcebus rufus*) in Eastern Madagascar. *Primates* **44:** 321–331.

de Ricqlès A, **Bourdon E**, **Legendre LJ**, **Cubo J. 2016.** Preliminary assessment of bone histology in the extinct elephant bird *Aepyornis* (Aves, Palaeognathae) from Madagascar. *Comptes Rendus Palevol* **15:** 197–208.

de Ricqlès A, **Padian K**, **Horner JR. 2001.** The bone histology of basal birds in phylogenetic and ontogenetic perspectives. In: Gauthier J, ed. *The Ostrom symposium.* New Haven: Yale University Press, 411–426.

Schweitzer MH, **Wittmeyer JL**, **Horner JR. 2005.** Gender-specific reproductive tissue in ratites and *Tyrannosaurus rex*. *Science* **308:** 1456–1460.

Starck JM, **Chinsamy A. 2002.** Bone microstructure and developmental plasticity in birds and other dinosaurs. *Journal of Morphology* **254:** 232–246.

Starck JM, **Ricklefs RE. 1998.** *Avian growth and development. Evolution within the altricial-precocial spectrum.* New York: Oxford University Press.

Steel L. 2009. Bone histology and skeletal pathology of two recently extinct flightless pigeons: *Raphus cucullatus* and *Pezophaps solitaria*. *Journal of Vertabrate Paleontology* **29:** 185.

Stein K, **Sander PM. 2009.** Histological core drilling: a less destructive method for studying bone histology. Lithodendron: The Occasional Papers of Petrified Forest National Park 1. Methods. In: *Fossil preparation: proceedings of the first annual fossil preparation and collections symposium*. M. A. Brown, J. F. Kane & W. G. Parker, Petrified Forest, April 2008, 69–80.

Storer R. 1960. Adaptive radiation in birds. In: Marshall AJ, ed. *Biology and comparative physiology of birds.* New York: Academic Press, 15–55.

Tattersall I. 1987. Itampolo: two subfossil sites in Madagascar. *Journal of Vertebrate Paleontology* **7:** 342–343.

Turvey ST, **Green OR**, **Holdaway RN. 2005.** Cortical growth marks reveal extended juvenile development in New Zealand moa. *Nature* **435:** 940–943.

Watanabe J. 2018. Ontogeny of surface texture of limb bones in modern aquatic birds and applicability of textural ageing. *The Anatomical record* **301:** 1026–1045.

Wetmore A. 1967. Re-creating Madagascar's giant extinct bird. *National Geographic Magazine* **132:** 488–493.

Whitehead CC. 2004. Overview of bone biology in the egg-laying hen. *Poultry Science* **83:** 193–199.

Wiman C. 1935. Uber Aepyornithes. *Nova Acta Regiae Societatis Scientiarum Upsaliensi* **9:** 1–57.

Wiman C. 1937a. Etude sur le segment terminal de l'aile des *Aepyornis* et des *Mullerornis*. *Bulletin de l'Académie Malgache, Nouvelle Série* **20:** 101–105.

Wiman C. 1937b. On supernumerary metapodials in *Aepyornis*, the moas, and some other birds. *Proceedings of the Zoological Society of London B* **107:** 245–256.